Simulating Model for Soil Water and Heat Conditions

Description of the SOIL model

Per-Erik Jansson

Simulating Model for Soil Water and Heat Conditions

Description of the SOIL model

Per-Erik Jansson

Preface

This is an update of the third technical description of the SOIL water and heat model first distributed during september 1996. The present report represents a detailed technical description of the SOIL water and heat model. Compared with the technical report by Jansson (1991) it includes a number of model developments. The present report is also part of the help to the WinSOIL program version 1.2. In addition to this report the user of the model are recommended to use the help. Previous users manual provided for MS-DOS version of SOIL are only valid in some minor parts and consequently they are not recommended to be used in connection with the windows version of the model. Some information that still refers to the MS-DOS version in this report may be invalid.

A bibliography is presented representing reports and papers with examples of how the SOIL model has been used. The reference list only includes documents that are referred to in this report which are not found in the bibliography.

Those who are interested in copies of the soil model are referred to our internet server where from which the model is also distributed:

ftp://bgfserver.mv.slu.se/demo/soil.zip

or

http://www.mv.slu.se/ bgf/soil.htm.

A user group is defined at majordomo@pinus.slu.se. If you want to join this group and obtain information on new version of the model please send an e-mail to: majordomo@pinus.slu.se and include the text: SUBSCRIBE SOILUSER NAME@XXX.XX

Uppsala 11 May, 1998

Per-Erik Jansson

Table of Contents

1.Introduction

1.1 Purpose of using the SOIL model

A number of problems concerning hydrological and/or thermal processes in the soil can be elucidated using the model. Both applied and basic scientific problems have been solved including:

- simulation of regulating factors for biological and chemical processes in the soil.
- assessment of the importance of different factors
- identification of gaps in our present knowledge
- formulation of new hypotheses
- generalisation of results to new soils, climates and time periods
- prediction of the influence of management e.g. soil heat extraction, mulching, drainage, irrigation and plant husbandry

1.2 Basic assumptions

The model, initially developed to simulate conditions in forest soils, has recently been generalised to elucidate water and heat processes in any soil independent of plant cover. This was possible since the model is based on well known physical equations. The fundamental nature of these physical equations allows the model to be adapted to many different types of ecosystems providing that we have quantitative knowledge of the governing properties of these systems.

The basic structure of the model is a depth profile of the soil. Processes such as snow-melt, interception of precipitation and evapotranspiration are examples of important interfaces between soil and atmosphere. Two coupled differential equations for water and heat flow represent the central part of the model. These equations are solved with an explicit numerical method. The basic assumptions behind these equations are very simple.

1) The law of conservation of mass and energy

2) Flows occur as a result of gradients in water potential (Darcy's Law) or temperature (Fourier's law).

1.3 Example of inputs

The soil profile is divided into a number of layers and for each layer, and each boundary between layers, these two basic principles are considered. The number of layers and the thickness of each layer can be varied depending on accuracy requirements.

The calculations of water and heat flows are based on soil properties such as:

- the water retention curve
- functions for unsaturated and saturated hydraulic conductivity
- the heat capacity including the latent heat at thawing/melting
- functions for the thermal conductivity

Water retention and unsaturated conductivity for a clay soil is illustrated in Figure 1.
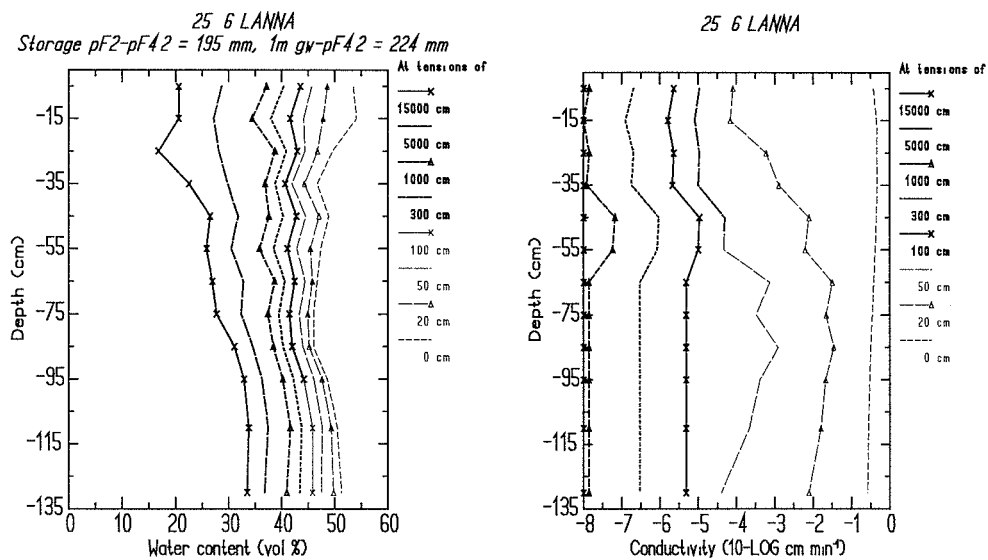
Figure 1. Physical soil properties of the Lanna clay soil, water retention (left) and unsaturated hydraulic conductivity (right). *Fysikaliska markegenskaper för lerjord vid Lanna, vattenbindning (till vänster) och omättad konduktivitet (till höger).*

The most important plant properties are:

- development of vertical root distributions
- the surface resistance for water flow between plant and atmosphere during periods with a non limiting water storage in the soil
- how the plants regulate water uptake from the soil and transpiration when stress occurs
- how the plant cover influences both aerodynamic conditions in the atmosphere and the radiation balance at the soil surface.

An example how the surface resistance may vary during the development of a crop is illustrated in Figure 2.

10

Surface resistance - barley crop

RSV(1)=140

RSV(3)=140

CFORM(2)=2

CFORM(1)=0 5

RSV(2)=40

DAYNUM(1)=121   DAYNUM(2)=175   DAYNUM(3)=242

Resistance (sm⁻¹)

150
125
100
75
50
25
0

May   Jun   Jul   Aug   Sep
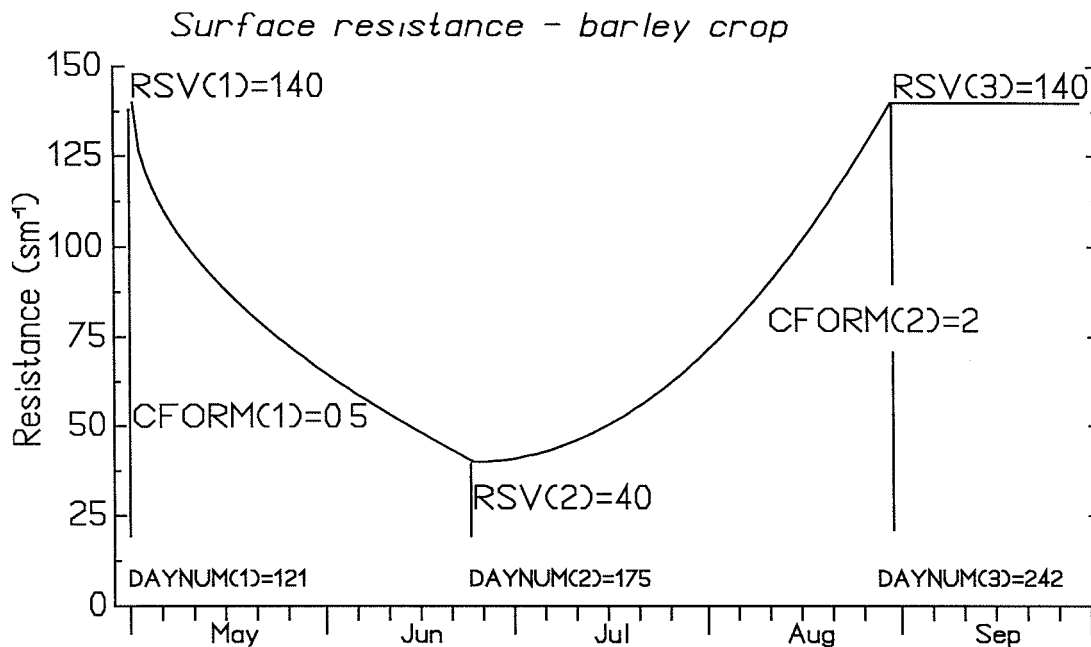
Figure 2. The surface resistance for a barley crop as specified by a set of parameter values.
Ytresistansens för en korngröda enligt angivna parametervärden

All properties are represented as parameter values. Numerical values are assigned to a number of different parameters representing properties of the soil-plant-atmosphere system. For each parameter a certain range reflects differences between different types of crops, forests, soils or the range reflects a typical variation found within a certain area.

Meteorological data are the driving variables to the model, but in contrast to parameters the numerical values of driving variables vary with time.

The driving variables govern the flows at the boundaries between atmosphere and soil and between plant and atmosphere. Most important of those are precipitation and air temperature (see Fig. 3) but air humidity, wind speed and cloudiness are also of great interest due to their influence on evaporation.

Precipitation (mm)

30

25

20

15

10

5

0

May   Jun   Jul   Aug   Sep   Oct   Nov   Dec   Jan   Feb   Mar   Apr

20

15

10

5

0

−5

−10

−15

−20

Temperature (°C)

May   Jun   Jul   Aug   Sep   Oct   Nov   Dec   Jan   Feb   Mar   Apr
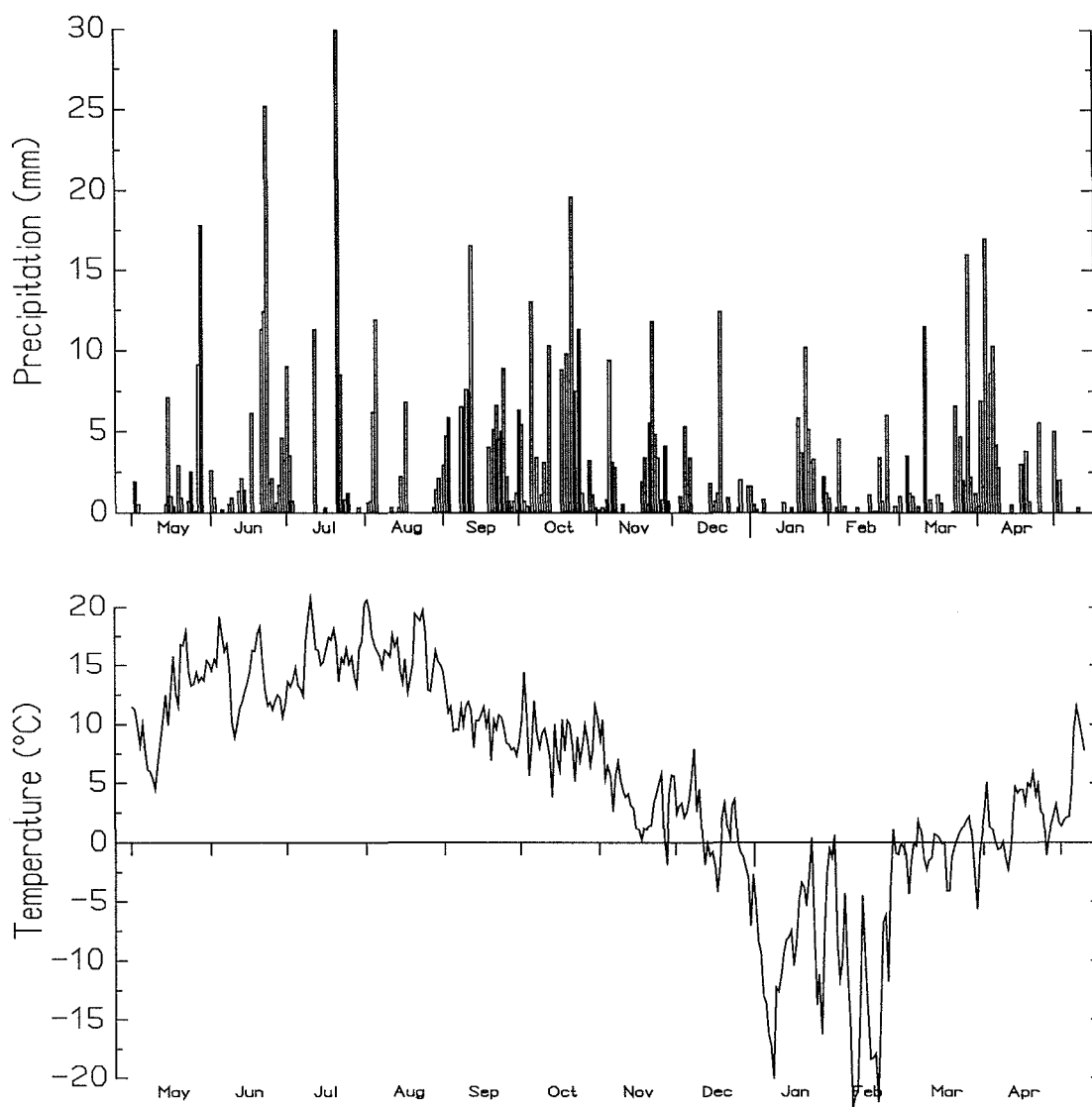
Figure 3. Daily values of precipitation and air temperature for one year. Dagliga värden av nederbörd och lufttemperatur för ett år.

The essential input data for running the model is stored in data bases accessible using interactive graphical programmes. Separate data bases for climate data and soil properties are available on IBM- PC standard diskette format.

The required information on soil properties is large compared to what is normally available from standard field investigations. To determine these properties by independent measurements in each application with the model would be time-consuming and very labour intensive, especially since some of these properties (e.g. hydraulic conductivity) show substantial spatial heterogeneity. The use of the data base enables the user to estimate a reasonable range for such soil properties from commonly available information such as soil texture and organic matter content. Most of the material in the data base originates from investigations in arable land in Sweden but the material is continuously updated with new sites including forest soils.

Figures 1 - 3 are examples of graphical representations of input data to the model. The graphic features are an integrated part of the data base programmes and plotting can be done on all standard graphic monitors such as CGA, EGA, VGA and Hercules as well as by printing devices which support any dot or vector based graphic standard.

1.4 Example of Outputs

Results of a simulation are obtained as time series either of variables which represent individual layers in the soil such as:

- temperature
- content of ice
- content of unfrozen water
- water potential
- vertical and horizontal flows of heat and water
- water uptake by roots
- storage's of water and heat
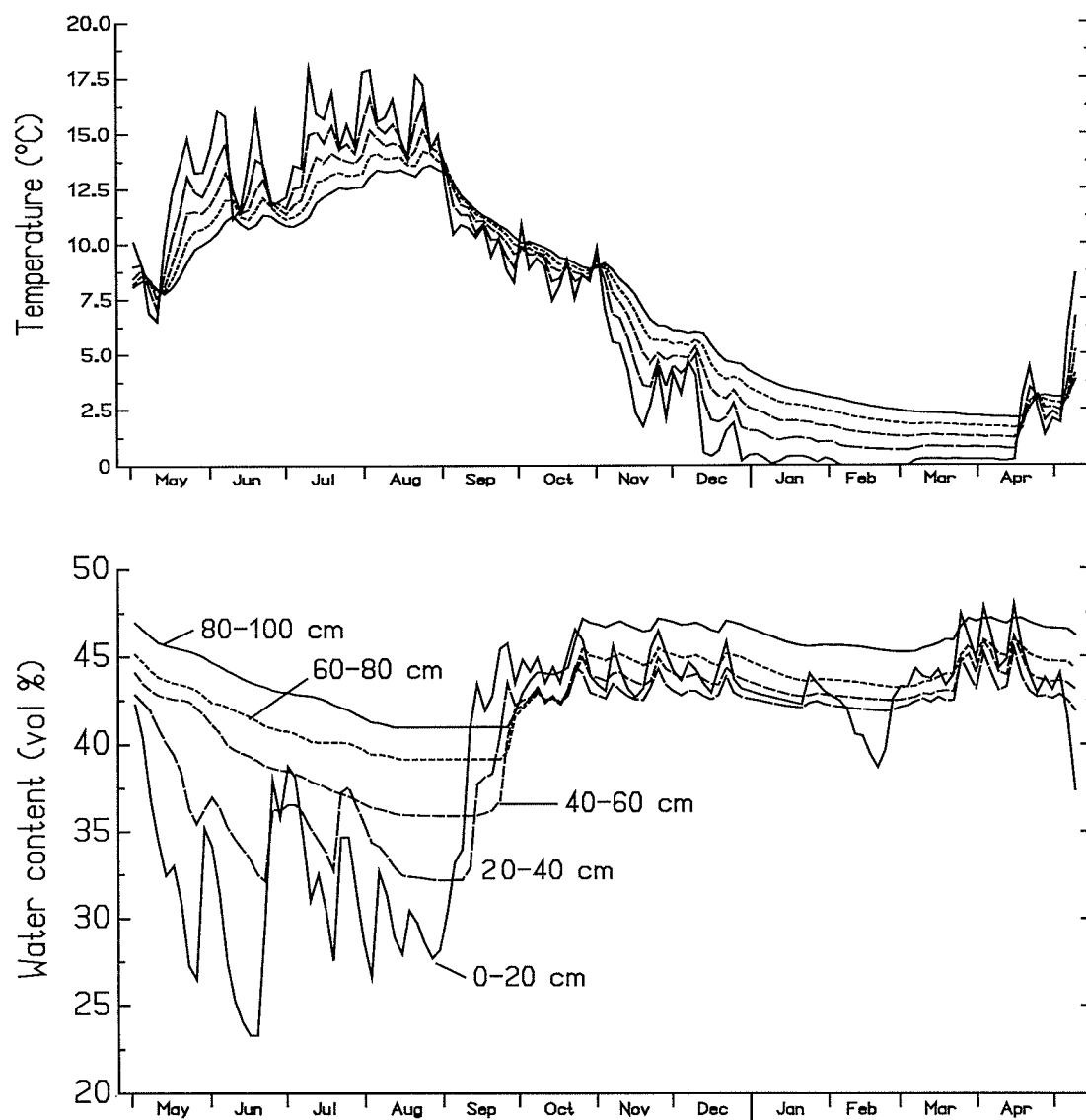
Figure 4. Simulated soil temperature and soil water content at different levels in a soil profile. *Simulerad marktemperatur och markvattenhalt för olika djup i en markprofil.*

13

In addition some output variables are represented as a single variable such as:

- snow depth
- water equivalent of snow
- frost depth
- surface runoff
- drainage flow
- deep percolation to ground water
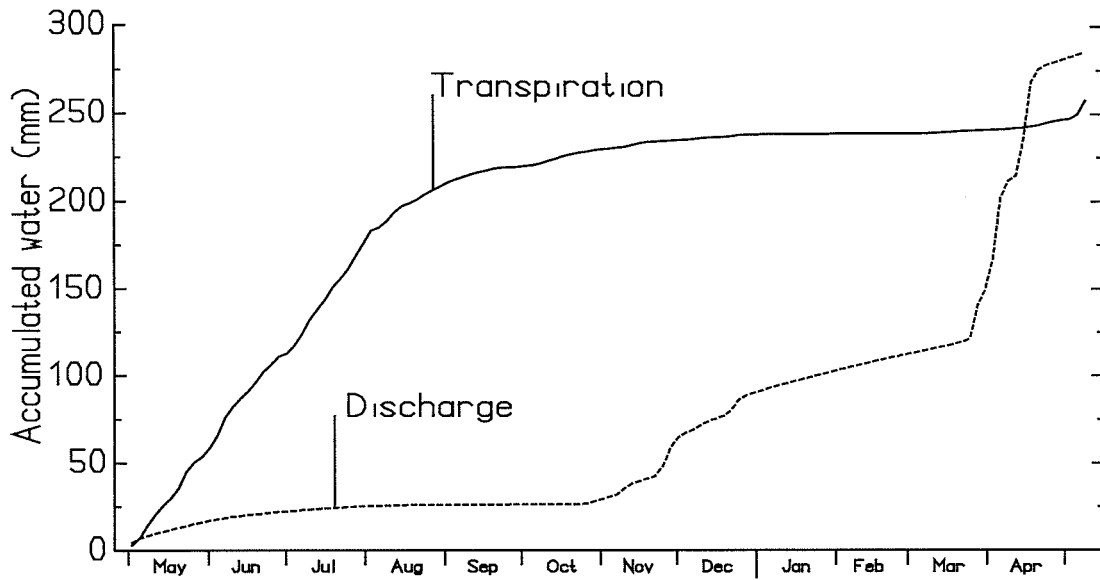
Figure 5. Simulated transpiration and discharge. Ackumulerade summor av simulerad transpiration och dränering.
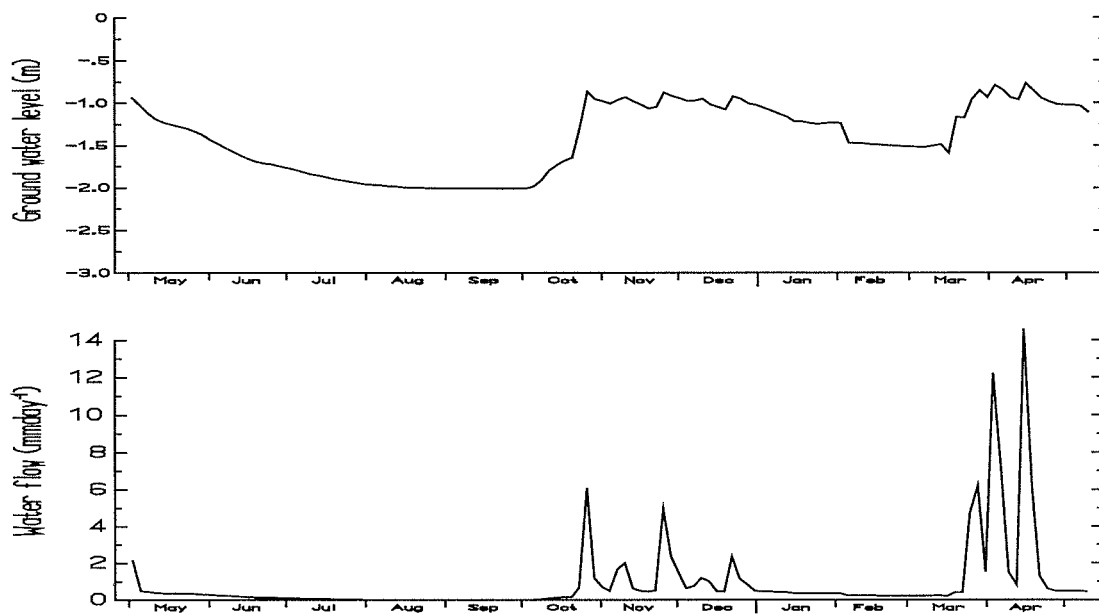
Figure 6. Simulated ground water level and discharge (tile drains at 1 m depth). *Simulerad grundvattenyta och dräneringsflöde genom dräneringsrör på 1 meters djup.*

It is a well known fact that no simulation model yields better results than can be expected from the quality of input data. Assessment of the uncertainty in the input data is therefore the first step when the model is to be used. Sometimes field measurements are available which enable a quantitative test of the model. The interpretation of discrepancies found between the measurements and the model predictions requires a lot of care and a basic knowledge of the different processes in the system. An improvement of the fit can normally be obtained after adjustments of some soil or plant properties. Nevertheless, it is not always the case that all input data including the physical properties of the system are correctly estimated just because a good fit is obtained when testing the model.

Figure 4 - 6 gives examples of typical results from model predictions in a standard application with an agricultural crop on a clay soil. Note that we can always simulate a much more complete picture of both the temporal pattern and of the interaction between variables than can be achieved by intensive field measurements. However, this should not lead us to believe more in the model predictions than in observations of the real system. Instead we have to design our field measurements to achieve an optimum test of the simulated results. We should concentrate on variables which are easy to measure and which have a strong connection to other variables in the soil-plant-atmosphere system. A typical example is soil water tension, which is easy to measure with a conventional tensiometer, but in addition reflects other factors such as soil water flow and water uptake by roots. Unsaturated water flows are very difficult to measure in field soils and in this case we must always rely on model predictions. However, tracers can be used as indicators of the actual water flow paths in the soil.

1.5 Experiences from model use

The model is helpful in elucidating how different processes and properties in the system interact. We are always constrained to investigate a limited part of the whole system with respect to both time and space. The model can be used as a tool to extend our knowledge.

The fundamental physical equations are well known and accepted but we still have to test their validity at different field scales. A general problem is that our knowledge of soil properties normally originates from small soil samples. The role of small soil units compared to larger units is not well understood and we have to find out how we can combine information which represents different scales. Areal mean values of soil properties such as the hydraulic conductivity are hard to determine even from intensive measurement programmes and it is not certain that the use of an areal mean will be the best choice for the model simulations.

One important aspect when testing the model is that parameter values should ideally have been estimated independently of the field measurements which are used to test the model predictions. In such a case we will learn about how the system behaves even when model predictions fail. On the other hand we will seldom learn about how nature behaves by using calibration procedures even if good agreements between simulated and observed variables are obtained. The estimated parameter values which result in a good agreement must always be compared with other independent estimates if a model application is to have scientific interest.

1) Do not be happy just because the model output is in agreement with observations; try instead to find out why there are no discrepancies.

2) Be happy when the model and the reality are different; then you have a key to new knowledge.

3) The model can provide you with a much better answer to an applied question than is possible with many field investigations. In many cases we cannot wait for the results from long term field investigations.

4) An adviser using a good mathematical model will certainly be efficient if he/she is successful in combining the results from the model with critical thinking. The model will stimulate an examination of problems if the adviser as well as the scientist gets an opportunity to play with the model.

5) An adviser who believes too much in the figures from a mathematical model will be equally poor as the one who fully trusts results from field investigations.

2. Theory and structure of model
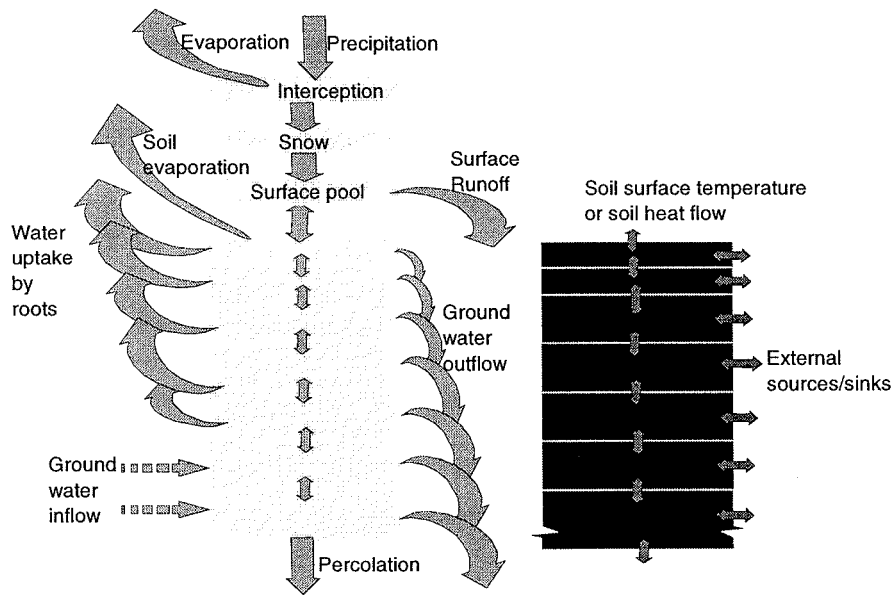
Figure 7. Mass balance (left) and heat balance (right) of the SOIL model. *Vattenflöden (till vänster) och värmeflöden (till höger) i SOIL modellen.*

The SOIL model represents, in one dimension, water and heat dynamics in a layered soil profile covered with vegetation. As the solution to model equations is performed with a finite difference method, the soil profile is divided into a finite number of layers (Fig. 7). Compartments for snow, intercepted water and surface ponding are included to account for processes at the upper soil boundary. Different types of lower boundary conditions can be specified including saturated conditions and ground water flow. In this chapter, the underlying concepts and equations are described for each component of the model.

2.1 Soil heat flow

Heat flow is the sum of conduction and convection:

$$q_h = -k_h \frac{\partial T}{\partial z} + C_w T q_w + L_v q_v \tag{1}$$

where the indices h, v and w mean heat, vapour and liquid water, q is flow, k is the conductivity, T is the temperature, C is the heat capacity, L is latent heat and z is depth. The convective term may be included or not in the solution depending on whether the switch HEATWF is put ON or OFF. Normally the convective term is important at high flow rates as during heavy snow melt infiltration. The general heat flow equation is obtained when combining Eq. (1) with the law of energy conservation:

$$\frac{\partial(CT)}{\partial t} - L_f \rho \frac{\partial \theta_i}{\partial t} = \frac{\partial}{\partial z}\left(k \frac{\partial T}{\partial z}\right) - C_w T \frac{\partial q_w}{\partial z} - L_v \frac{\partial q_v}{\partial z} - s_h \tag{2}$$

where indices i and f mean ice and freezing respectively, t is time, ρ is density,: L is latent heat, θ is the volumetric water content, and s is a source/sink term. The two terms on the left represent changes in sensible and latent soil heat contents, and the last term to the right accounts for, e.g., the soil heat exchange of a heat pump system.

2.1.1 Heat capacity, unfrozen conditions

Soil heat capacity equals the sum of heat capacities of soil constituents. Solid soil constituents are given on a volumetric basis. Heat capacity of air is negligible, such that:

$$C = f_s C_s + \theta C_w \tag{3}$$

where index f_s is the volumetric fraction of solid soil material including mineral and organic matter. C_s and C_w are heat capacities for solid material and water, respectively. C, here given for unfrozen soil, can also be computed for a frozen soil (cf. Eq. (18)). C is never explicitly given for a partly frozen soil since temperature, in this case, is obtained by special calculations (see Eqs. (19) - (25)).

2.1.2 Thermal conductivity, unfrozen conditions

Thermal conductivity is a complex function of soil solids and soil moisture. For humus, i.e., organic matter, the thermal conductivity function is adapted from a figure in de Vries (1975):

$$k_{ho} = h_1 + h_2 \theta \tag{4}$$

where h_1 and h_2 are empirical constants. For unfrozen mineral soil an empirical conductivity function is adapted from Kersten (1949):

$$k_{hm} = 0.143\left(a_1 \log\left(\frac{\theta}{\rho_s}\right) + a_2\right)10^{a_3 \rho_s} \tag{5}$$

where a_1, a_2, a_3 are constants and ρ_3 is the dry bulk soil density (Fig. 8). The logarithmic argument, θ/ρ_s, is equivalent to the soil water content expressed on a mass basis.

18
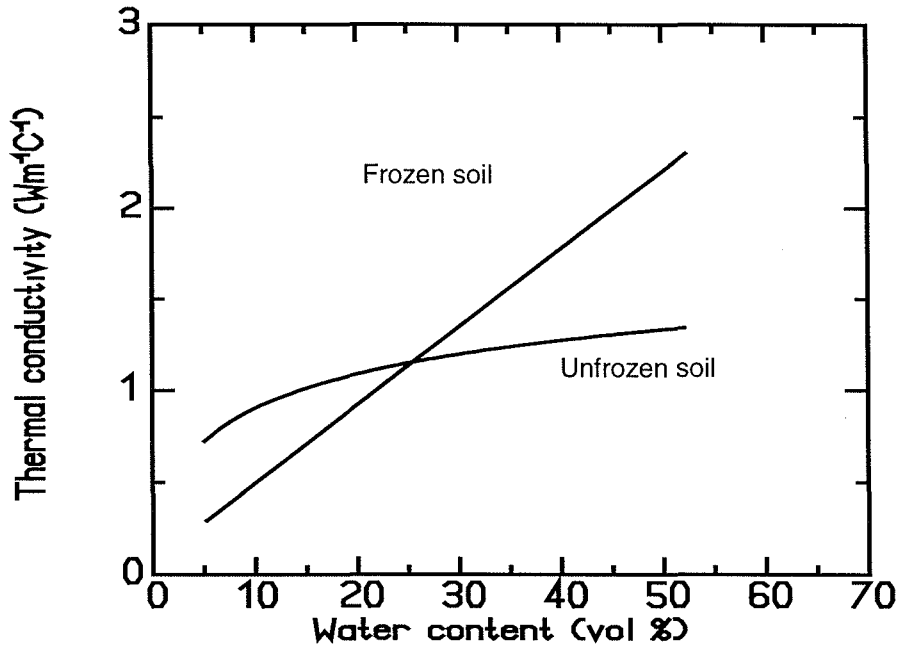
Figure 8. Thermal conductivity. Kersten's equations, originally given for water content in percent by weight, are here recalculated to volumetric basis for a specific soil. *Värmeledningsförmåga enligt Kerstens ekvationer.*

2.1.3 Upper boundary condition

The upper boundary condition can be specific in different ways. If soil surface temperature, T_s, is not measured, the simplest way (where the switch SUREBAL is put OFF) is to assume for snow free periods that:

$$T_s = T_a \tag{6}$$

where the indices s and a mean surface and air respectively. If the interaction between aerodynamic properties, plant cover and surface evaporation is of interest, the surface temperature may also be calculated by solving the heat flow equation at the soil surface (The switch SUREBAL is put ON). This physical approach is described in the section 0 which is also relevant for the boundary condition for the water flow equations.

2.1.3.1 Influence of snow

For periods with snow cover, soil surface temperature is given by assuming steady state heat flow (see Fig. 9) between the soil and a homogeneous snow pack:

$$T_{ss} = \frac{T_1 + aT_a}{1 + a} \tag{7}$$

where the index 1 means the top soil layer, and the snow surface temperature is assumed to obey Eq. (6). The weighting factor, a, is given by:

19

$$a = \frac{k_{snow}\left(\frac{\Delta z_1}{2}\right)}{k_h \cdot \Delta z_{snow}}$$ (8)

where Δz denotes thickness.

If the amount of liquid water in the snow pack (S_w) exceeds a constant threshold, S_{wlmin} , soil surface temperature, T_{ss} , is put equal to 0^oC.

$$q_h = k_{snow}\frac{T_A - T_{ss}}{\Delta z_{snow}}$$

$$q_h = k_h\frac{T_{ss} - T_1}{\frac{\Delta z_1}{2}}$$
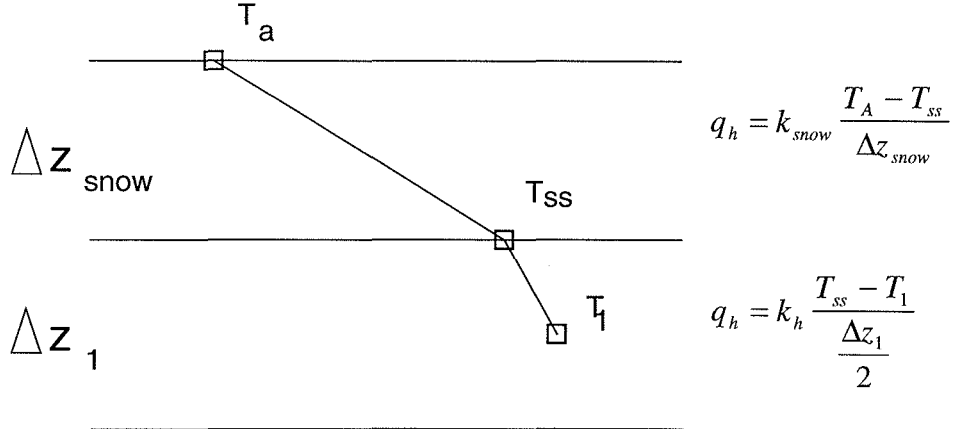
Figure 9. The steady state assumption of heat flow through the upper soil layer and the snow pack.
Antagandet om stationärt flöde genom snötäcket och det översta markskiktet.

During conditions when the snow depth is below a certain value Δz_{cov} the soil surface temperature will be calculated as a weighted sum between the calculated temperature below the snow and an estimated soil surface temperature from bare areas. The mean soil surface temperature is then given by:

$$T_s = (1 - \frac{\Delta z_{snow}}{\Delta z_{cov}})T_s + \frac{\Delta z_{snow}}{\Delta z_{cov}}T_{ss}$$ (9)

2.1.4 Mixed composition of top layer

Calculation of soil surface heat flow, q_h (0), requires special attention. Convective heat inflow is given by precipitation throughfall and/or snow melt multiplied by the relevant surface temperature and the heat capacity of liquid water (cf. Eq. (1)). Since thermal properties of humus and mineral soil differ markedly, special treatment is required for a thin humus layer when numerical requirements demand that the top compartment represents a layer thicker than the humus layer. Three special cases for heat conduction are given, depending on the depth of the insulating litter or humus layer.

For negligible depths, i.e., less than 5 mm, thermal conduction in humus is neglected:

$$q_h(0) = 2k_{hm} \frac{(T_s - T_1)}{\Delta z_1}$$
(10)

For a humus layer thicker than 5 mm but less than half the depth of the top soil layer a steady-state solution, analogous to the one for snow, gives the boundary temperature between humus and mineral soil:

$$T_b = \frac{T_1 + aT_s}{1+a}$$
(11)

where

$$a = \frac{k_{ho}(\Delta z_1 / 2 - \Delta z_{humus})}{k_{hm} \Delta z_{humus}}$$
(12)

This finally yields

$$q_h(0) = k_{ho} \frac{(T_s - T_b)}{\Delta z_{humus}}$$
(13)

For humus layers thicker than half the top soil layer, Eq. 12 degenerates into the standard solution, i.e.:

$$q_h(0) = 2k_{ho} \frac{(T_s - T_1)}{\Delta z_1}$$
(14)

2.1.5 Lower boundary condition

The lower boundary condition for heat conduction can be given as a temperature or as a constant flow which may be zero or equal to a constant geothermal contribution, q_h *(low)*. The temperature, $T(low)$ is calculated from the assumed values of mean air temperature T_{amean} and the amplitude of air temperature, T_{aamp} during the year (see Fig. 10) from, an analytical solution of the conduction equation.

$$T(z,t) = T_{amean} - T_{aamp} e^{-\frac{z}{d_a}} \cos\left((t - t_{ph})\omega - \frac{z}{d_a} \right)$$
(15)

where t is the time, t_{ph} is the phase shift, ω is the frequency of the cycle and d_a is the damping depth. The frequency is defined as:

$$\omega = \frac{2\pi}{y_{cycle}}$$ (16)

where y_{cycle} is the length of the period and the damping depth, d_a , is given as:

$$d_a = \sqrt{\frac{2D}{\omega}}$$ (17)

where D is the thermal diffusivity which is given as the ratio between the thermal conductivity, $k_{h,}$, and the heat capacity, C, of the soil at a moisture content that equals the selected initial conditions.
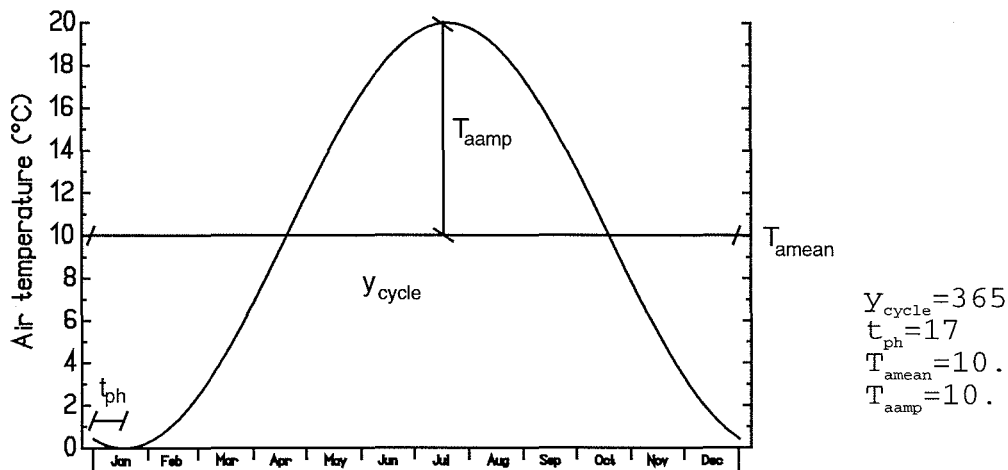
Figure 10. The air temperature calculated using a set of parameter values. *Lufttemperaturens variation under året beräknad med givna parametervärden.*

Heat convection at the lower boundary condition depends on the presence of a ground water table in the profile. For an unsaturated profile convection follows percolation from the lowest soil layer. When a horizontal net ground water flow is present, convection follows this flow and is neglected for all layers below ground water level.

2.2 Soil frost

Treatment of frost in the soil is based on a function for freezing point depression and on an analogy between processes of freezing-thawing and drying-wetting, i.e., the liquid-ice interface is considered equal to the liquid-air interface. Thus, unfrozen water below zero is associated with a matric potential and an unsaturated conductivity. Freezing gives rise to a potential gradient which in turn forces a water flow according to the prevailing conductivity. This causes a capillary rise of water towards the frost zone and it also allows drainage of snow melt through the frost zone when frozen soil temperatures are close to 0 °C.

2.2.1 Freezing point depression and heat capacity of frozen soil

The simplifying assumption is made that all water at the temperature, T_f is frozen except of a residual unfrozen amount, θ_{lf} calculated as:

$$\theta_{lf} = d_1\theta_{wilt} \tag{18}$$

where is a constant and θ_{wilt} is volumetric water content at a soil water potential corresponding to pF 4.2. For temperatures below T_f , heat flows and temperatures are calculated in analogy with unfrozen conditions. For temperatures between 0 °C and T_f a soil heat capacity is first calculated:

$$C_f = f_s C_s + \theta_i C_i + \theta_{lf} C_w \tag{19}$$

This is used to calculate heat content of soil, E_f, at the temperature T_f:

$$E_f = C_f T_f - L_f w_{ice} \tag{20}$$

Where w_{ice} is the mass of water available for freezing which is calculated as:

$$w_{ice} = w - \Delta z \theta_{lf} \rho_{water} \tag{21}$$

where w is the total mass of water.

Relative fraction of latent heat of ice to the total heat content of soil is given at T_f by :

$$f_{lat} = \frac{L_f w_{ice}}{E_f} \tag{22}$$
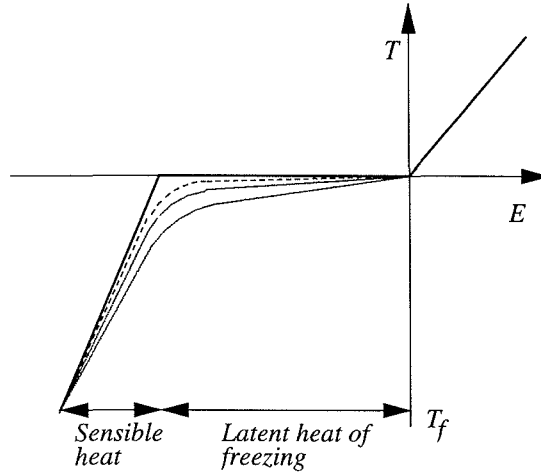
Figure 11. Soil temperature (T) as a function of heat content (E) for different degrees of freezing point depression, i.e., different values of $d_2\lambda+d_3$ (see Eq. (23)). Both axes are distorted for the sake of clarity. With a completely frozen soil temperature (T_f) of -5° C the ratio between sensible and latent heat is approximately 1:24. *Marktemperatur som en funktion av värmeinnehåll för olika värden av $d_2\lambda+ d_3$. Axlarna är ej skalenliga. För en helt frusen jord så är relationen ungefär 1:24 mellan sensibel och latent energi.*

Freezing point depression, which depends on soil texture (Fig. 11), is then expressed by the ratio between latent heat contents of E at temperature $T(0 > T > T_f)$ and E_f

at temperature T_f:

$$r = \left(1 - \frac{E}{E_f}\right)^{d_2\lambda+d_3} \min\left(1, \frac{E_f - E}{E_f + L_f w_{ice}}\right)$$ (23)

where d_2 and d_3 are empirical constants and λ is the pore size distribution index (cf. Eq. (41)). The second term in Eq. (23) is inserted to ensure that temperatures close to t_f never exceed free water temperatures at equivalent heat contents. Sensible heat content, H, is given by:

$$H = E(1 - fL_{lat})(1 - r)$$ (24)

Temperature is finally achieved as a function of sensible heat content:

$$T = \frac{H}{C_f}$$ (25)

When the upper boundary condition is given as a measured temperature of the uppermost layer and the temperature corresponds to a partially frozen soil $(T_f < T < 0)$, the heat content, E_l, is calculated from the temperature, T_l. This is accomplished through an approximate inversion of Eq. (23):

$$E_1 = L_f w \left(\frac{T_1}{T_f} \right)^{\left(\frac{\lambda d_3 + d_2}{d_2 d_3} \right)} + C_i T_1 \qquad (26)$$

2.2.2 Thermal conductivity, frozen soil

Thermal conductivity of a fully frozen organic soil is calculated with a similar equation as for unfrozen organic soils but including a second degree coefficient to account for the influence of ice on the conduction in the soil.

$$k_{ho}(frozen) = \left(1 + 2Q \left(\frac{\theta}{100} \right)^2 \right) k_{ho}(unfrozen) \qquad (27)$$

where Q is the thermal quality of the soil layer (see eq. 30).

Thermal conductivity of fully frozen mineral soil (Fig. 8) is adapted from Kersten (1949):

$$k_{hi} = b_1 10^{b_2 \rho_s} + b_3 \left(\frac{\theta}{\rho_s} \right) 10^{b_4 \rho_s} \qquad (28)$$

where b_1 to b_4 are empirical constants. For temperatures between 0 °C and T_f a weighted conductivity is used:

$$k_h = Q k_{hi} + (1 - Q) k_{hw} \qquad (29)$$

where the thermal quality, Q, (the mass ratio of frozen water to total amount of water) is deduced from energy relations:

$$Q = -\frac{(E - H)}{L_f w_{ice}} \qquad (30)$$

2.2.3 Frost boundary

For purposes of model output frost boundaries are calculated in a separate subroutine as isotherms of 0° C. The somewhat less realistic assumption of linear heat variations with depth between discrete layers give these isotherms a strong dependence on compartmentalisation. Not more than two frost layers are allowed for output purposes.

2.2.4 Influence of ice on water flows

Two different calculations are made in the model to reduce the hydraulic conductivity under partially frozen conditions. The interpolation procedure for obtaining the boundary conductivity between two layers may optionally (see section "switches" in user's manual) be replaced by a procedure in which the boundary conductivity is selected as the minimum conductivity of the two layers. This will normally substantially reduce the flow towards the layer where freezing is taking place and the clear tendency to overestimate redistribution during freezing will be reduced (Lundin, 1990).

In addition to the alternative interpolation procedure an impedance factor is considered when the hydraulic conductivity of a partially frozen layer, k_{wf}, is calculated:

$$k_{wf} = 10^{-fc_iQ} k_w \qquad (31)$$

where Q is the thermal quality, fc_i is an impedance parameter and k_w is the hydraulic conductivity of the layer calculated from the unfrozen water content without accounting for occurrence of ice.
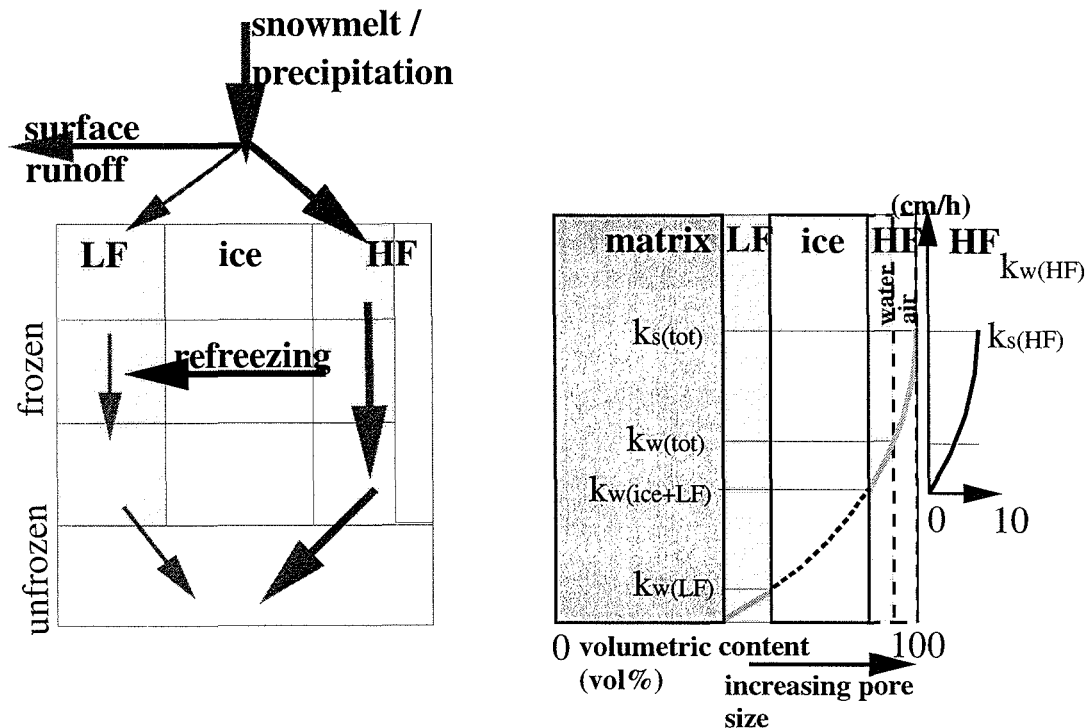
Figure 12. The flow paths and the hydraulic conductivities for the two domain approach. (After Stähli et al, 1996)

A two domain approach was introduced in the model by Stähli et al. (1996) after suggestions from Johnsson & Lundin (1991). The new approach separates between one low flow domain which is the same as used previously when estimating water flows in the partially unfozen soil and a high flow domain (see Figure 12). The high flow domain allows rapid flow of infiltrating water provided that air filled pores were present at time of infiltration. The flow in the high flow domain is based on a unit gravitational gradient and the hydraulic conductivity, k_{hf}:

$$k_{hf} = k_w(\theta_{tot}) - k_w(\theta_{lf} + \theta_{ice}) \qquad (32)$$

where $k_w(\theta_{tot})$ is the hydraulic conductivity corresponding to all volume occupied by water and $k_w(\theta_{lf}+\theta_{ice})$ is the hydraulic conductivity corresponding to the volume occupied by water and ice in the low flow domain.

At the soil surface, water may infiltrate into the low flow domain until the capacity of this domain in reached, i.e. the unsaturated conductivity $k_w(\theta_{lf})$ times the total water potential gradient. The surplus water enters the air filled pores to a degree that is limited to the conductivity of the high flow domain (k_{hf}). If also the capacity of the high flow domain is reached by the snow melt or precipitation the surface pool will receive an input of water.

Water infiltrating in the high flow domain is assumed to have a temperature close to 0 °C. As it percolates through the high flow domain, it may refreeze to a certain degree depending on the soil temperature. The heat which is released from freezing in the high flow domain causes melting of ice in the finest ice filled pores, shifting the boundary between the low flow domain and the ice domain toward larger pores. Thus, refreezing of infiltrating water is treated as a redistribution $(q_{infreeze})$ from the high flow to the low flow domain:

$$q_{\inf reeze} = \alpha_h \Delta z \frac{T}{L_f} \tag{33}$$

where α_h is a heat transfer parameter, Δz is the thickness of the layer, T is the temperature of the layer and L_f is the latent heat of freezing.

2.2.5 Frost heaving

Frost heave is optionally treated (see section "switches" in user's manual) in a simplistic way. A soil compartment will heave if the total volume of ice and unfrozen water exceeds the porosity of the soil in a layer.

2.3 Soil water flow

Water flow in the soil is assumed to be laminar and, thus, obey Darcy's law as generalised for unsaturated flow by Richard (1931):

$$q_w = -k_w \left(\frac{\partial \psi}{\partial z} - 1 \right) - D_v \frac{\partial c_v}{\partial z} \tag{34}$$

where ψ is the water tension, c_v is the concentration of vapour in soil air and D_v is the diffusion coefficient for vapour in the soil. The general equation for unsaturated water flow follows from Eq. (34) and the law of mass conservation:

$$\frac{\partial \theta}{\partial t} = -\frac{\partial q_w}{\partial z} + s_w \tag{35}$$

where s_w is a source/sink term.

2.3.1 Bypass flow in macropores
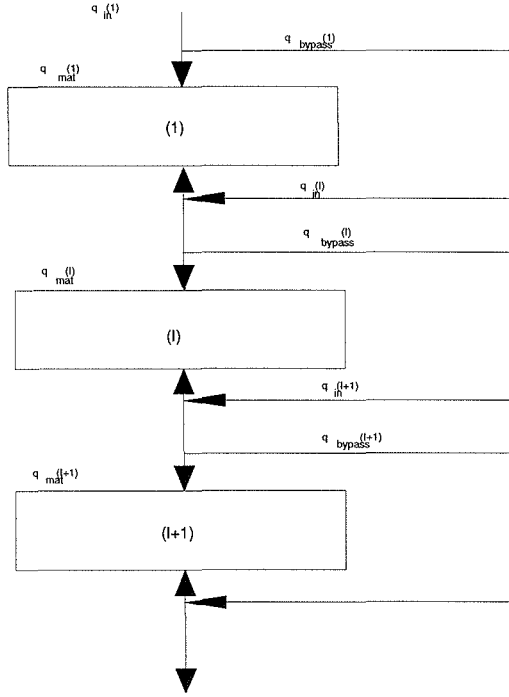
Figure 12 Water flow paths when bypass flows are considered. *Vattenflödesbanor vid förbipassage av markskikt.*

An optional switch (CRACK) to account for bypass flow has been included in the model to consider rapid flow in macropores during conditions when smaller pores are only partially filled with water (Fig. 12). The amount of water in the macropores is not accounted for explicitly. Instead, the infiltration flow rate at the soil surface or the vertical flow in the macropores at any depth in the soil profile, q_{in}, determines the partitioning into ordinary Darcy flow, q_{mat}, and bypass flow, q_{bypass}.

$$q_{mat} = \max\left(k_w(\theta)\left(\frac{\partial \psi}{\partial z} + 1\right), q_{in}\right) \qquad 0 < q_{in} < S_{mat} \qquad (36)$$

$$q_{bypass} = 0 \qquad\qquad\qquad 0 < q_{in} < S_{mat} \qquad (37)$$

$$q_{mat} = S_{mat} \qquad\qquad\qquad q_{in} \geq S_{mat} \qquad (38)$$

$$q_{bypass} = q_{in} - q_{mat} \qquad\qquad q_{in} \geq S_{mat} \qquad (39)$$

where $k(\theta)$ is the unsaturated conductivity at a given water content, ψ is the water tension and z is the depth co-ordinate. At the soil surface, q_{in} is the infiltration rate. At other depths in the soil, q_{in} is the vertical flow rate in the macropores (q_{bypass}) from the layer immediately above. S_{mat} is defined as:

$$S_{mat} = a_{scale} a_r k_{mat} pF \qquad\qquad\qquad\qquad (40)$$

where k_{mat} is the maximum conductivity of smaller pores (i.e. matrix pores), a_r is the ratio between compartment thickness and the unit horizontal area represented by the model, pF is $^{10}\log$ of ψ and a_{scale} is an empirical scaling coefficient accounting for the geometry of aggregates.

The calculated water flow in the matrix (q_{mat}) is used to update the water contents and the water tensions in the numerical solution, whereas q_{bypass} is directed without delay to the next soil compartment. However, q_{bypass} can never reach layers below the water table depth, which is the lower boundary condition for the use of Richard's equation.

2.3.2 Soil hydraulic properties

Two different soil hydraulic properties are important namely the water retention curve and the unsaturated conductivity function. Both properties are considered as unique functions of the water content with or without hysteresis effects. Figure 13 shows how experimental data of water retention can be used when estimating coefficients in the function proposed by Brooks & Corey (1964) which is used in an intermediate range of the water retention curve (see Fig. 14).
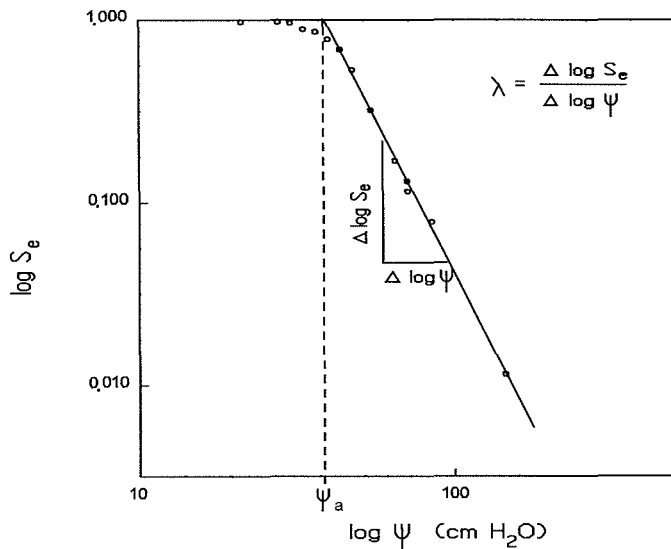
Figure 13. Log S_e as a function of log ψ. The air entry pressure (ψ_a) is given at S_e=1.0. Pore size distribution index (λ) is the slope of the line. *Grafisk återgivning av Brooks & Corey's samband i log-log diagram. Porstorleks-fördelningsindex (λ) fås genom lutningen av den räta linjen.*

The function by Brooks & Corey (1964) is given by:

$$S_e = \left(\frac{\psi}{\psi_a} \right)^{-\lambda}$$ (41)

where ψ_a is the air-entry tension and λ is the pore size distribution index. Effective saturation is defined as:

$$S_e = \frac{\theta - \theta_r}{\theta_s - \theta_r}$$ (42)

where θ_s is the porosity and θ_r is the residual water content. Calculation of the parameters λ, ψ_a and θ_r is done by least squares fittings of Eqs. (41) and (42) to experimental data, preferably from undisturbed soil cores or in situ measurements (see Fig. 13). Such experimental data usually yield a good fit over an intermediate range of tensions.

As an alternative expression to the Brooks & Corey expressions the equation by van Genuchten (1980) has been introduced:

29

$$S_e = \frac{1}{(1+(\alpha\psi)^{gn})^{gm}}$$

(43)

where α, gn and gm are empirical parameters.

In order to get a good fit in the whole range, Eqs. (41) and (42) are fitted only to data corresponding to tensions below a threshold value, ψ_x. The relation between water content and tension above this threshold is assumed log-linear:

$$\frac{\log\left(\frac{\psi}{\psi_x}\right)}{\log\left(\frac{\psi_{wilt}}{\psi_x}\right)} = \frac{\theta_x - \theta}{\theta_x - \theta_{wilt}} \qquad \psi_x < \psi < \psi_{wilt} \qquad (44)$$

where θ_x ($=\theta(\psi_x)$) is the threshold water content and θ_{wilt} is the water content at wilting point, defined as a tension of 15 000 cm water.

In the range close to saturation, i.e. from θ_s to θ_m a linear expression is used for the θ - ψ relationship.

$$\psi = \psi_m - \frac{(\theta - \theta_s + \theta_m)}{\theta_m} \psi_m \qquad (45)$$

where ψ_m is the tension which corresponds to a water content of θ_s - θ_m. The three different parts of the water retention curve is illustrated for a sandy soil below (Fig. 14.)
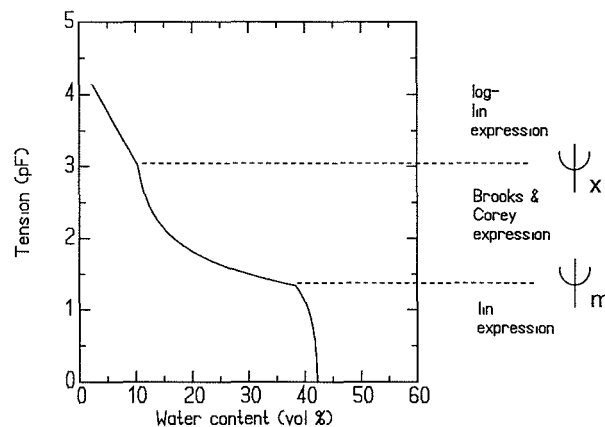
Figure 14. An example of how three different expressions in the water retention curve are used in different ranges. The pF value corresponds to the logarithm of tension expressed in cm. *Ett exempel på hur 3 olika uttryck används för att beskriva pF-kurvan. pF motsvarar logaritmen av tensionen uttryckt i cm vattenpelare.*

Following Mualem (1976), and using the analytical expressions according to Brooks & Corey (41) and (42), the unsaturated conductivity is given by:

$$k_w = k_{mat} S_e^{\left(n+2+\frac{2}{\lambda}\right)} \tag{46}$$

and

$$k_w = k_{mat}\left(\frac{\psi_a}{\psi}\right)^{2+(2+n)\lambda} \tag{47}$$

k_{mat} is saturated conductivity and n is a parameter accounting for pore correlation and flow path tortuosity. Eqs. (41) and (42) are used for water contents in the matrix pores. In case of using the van Genuchten equation the corresponding equation for the unsaturated conductivity is given by:

$$k_w = k_{mat} \frac{\left(1-(\alpha\psi)^{gn-1}\left(1+(\alpha\psi)^{gn}\right)^{-gm}\right)^2}{\left(1+(\alpha\psi)^{gn}\right)^{\frac{gm}{2}}} \tag{48}$$

where the coefficients a, gn and gm are the same as used in eq. (43).

$k_{sat}=0.0260\ cm\ min^{-1}$

$k_{mat}=0.0001\ cm\ min^{-1}$

$\theta_s=53.5$

$\theta_r=12.2$

$\lambda=0.4$

$\psi_a=256\ cm\ water.$

$n=1$
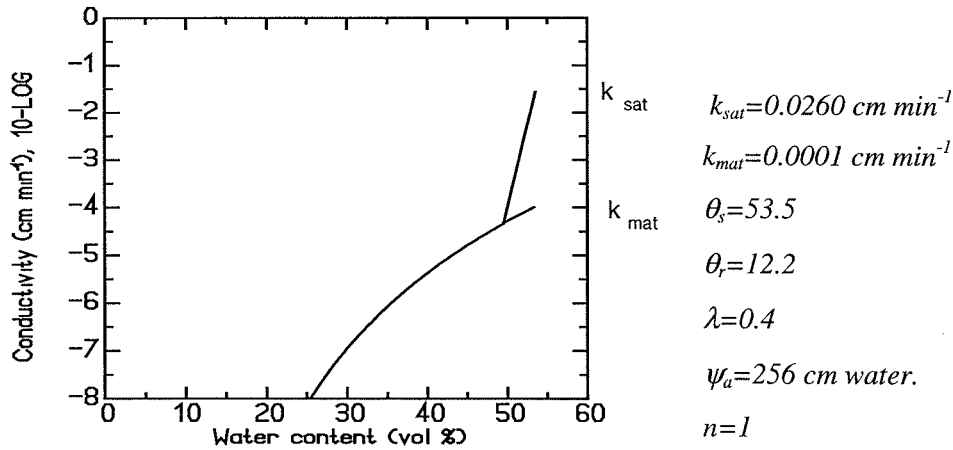
Figure 15. The unsaturated conductivity for a clay soil calculated with the parameter values given above. *Omättad konduktivitet beräknad för en lerjord med angivna parametervärden.*

To account for the contribution of macropores, an additional contribution to the hydraulic conductivity is considered when water content exceeds $\theta_s - \theta_m$ (see Fig. 15.).

$$k_w = 10^{\left(\log(k_w(\theta_s-\theta_m)) + \frac{\theta-\theta_s+\theta_m}{\theta_m}\log\left(\frac{k_{sat}}{k_{w(\theta_s-\theta_m)}}\right)\right)} \tag{49}$$

where k_{sat} is the saturated conductivity which includes the macropores k_w $(\theta_s - \theta_m)$ is the hydraulic conductivity calculated from Eqs. (46-48).

31

All the hydraulic conductivies are scaled with respect to temperature effects which are simplified to a linear response in the normal range from 0 °C to 20 °C which is the reference temperature used. In addition to this dependence which is related to the viscosity of water also a minimum unsaturated conductivity is applied. Thus the conductivity is given by:

$$k_w = (r_{AOT} + r_{A1T}T_s)\max(k_w^*, k_{\min uc}) \qquad (50)$$

where r_{AOT}, r_{A1T} and k_{minuc} are parameter value. K_w^* is the conductivity according to Eqs. (46-49).

2.3.3   Hysteresis effects on soil hydraulic properties

The hysteresis may be assumed in the water retention curve and in the unsaturated conductivity function depending on the switch HYSTERES.

The calculation of hysteresis is based on three multiplicative functions considering the time since start of sorption loop (R_{hage}), the shift point pF-value (R_{hshift}) and the accumulated rate of water content increase (R_{hacc}). These three functions are governed by common parameter values for all layers and they can all vary between zero and unity. In addition for each layer one parameter p_{hysmax} gives the maximal effect

Thus

$$\psi = \psi^* 10^{R_h P_{hys\,max}} \qquad (51)$$

where ψ^* is the reference value of water tension, and R_h is the hysteresis effect calculated as:

$$R_h = R_{hage} R_{hshift} R_{hacc} \qquad (52)$$

The age response is given as:

$$R_{hage} = e^{-a_{hysk}\Delta t_{shift}} \qquad (53)$$

where Δt_{shift} is the time elapsed since last major shift from a desorption to a sorption process.

The shift point response is:

$$R_{hshift} = \max\left(R_{hage}, \min\left(\frac{\log\psi - a_{PF1}}{a_{PF2} - a_{PF1}}, 1\right)\right) \qquad (54)$$

and finally the accumulated change of water content is defined as:

$$R_{hacc} = \min\left(1, \frac{\Delta\theta_{sorp}}{a_{thetm}}\right) \qquad (55)$$

where the $\Delta\theta_{sorp}$ is the accumulated increase of water content at a rate that exceeds the threshold value $a_{\theta D}$

since the last major shift from desorption to sorption. The $\Delta\theta_{sorp}$ is reset to a value that corresponds to continuos change in the total hysteresis response when a new sorption process starts.

Similar as for the water tension the hydraulic conductivity is given as:

$$k_w = k_w^* \, 10^{R_h P_{hys\,max\,c}} \qquad (56)$$

2.3.4 Water vapour flow

The soil vapour flux was introduced as a switch (VAPOUR) which includes the vapour flow as an optional contribution to both the water and energy flow in the soil (se Eqs. 1 and 34).

Vapour flows between adjacent soil layers will be calculated from gradients in vapour pressure and diffusion coefficient. The diffusion coefficient is adjusted because of deviations from diffusion in free air by use of a parameter (d_{vapb}). The vapour flow is given by:

$$q_v = -d_{vapb} f_a D_0 \frac{\partial c_v}{\partial z}$$
(57)

where f_a is the fraction of air filled pores, D_0 is the diffusion coefficient in free air which is given as a function of the soil temperature as:

$$D_0 = \left(\frac{T + 273.15}{273.15} \right)^{1.75}$$
(58)

c_v is the vapour concentration which is given by the vapour pressure. Thus:

$$c_v = \frac{M e_v}{R(T + 273.15)}$$
(59)

where M is the molar mass of water, R is the gas constant, T is the soil temperature and the vapour pressure (e_v) is given by:

$$e_v = e_s e^{\left(\frac{\frac{-\psi}{100} Mg}{R(T+273.15)} \right)}$$
(60)

where e_s is the vapour pressure at saturation and ψ is the soil water tension. The later expression is used from the basic assumption that the liquid phase is in equilibrium with the gas phase in the soil.

2.3.5 Upper boundary condition

Boundary conditions at the soil surface are given by separate subroutines accounting for snow melt and interception of precipitation by vegetation.

Water coming from snow or from precipitation infiltrates into the soil providing that the infiltration capacity is high enough. Otherwise a surface pool of water will be formed on the soil surface. Water in the surface pool can either infiltrate with a delay into the soil or be lost as surface runoff. The surface runoff, q_{surf}, is calculated as a first order rate process:

$$q_{surf} = a_{surf} (W_{pool} - w_{p\max})$$
(61)

where a_{surf} is an empirical coefficient, W_{pool} is the total amount of water in the surface pool and w_{pmax} is the maximal amount which can be stored on the soil surface without causing any surface runoff.

The fraction of the total soil surface that is covered with water (f_{cspool}) is given by:

$$f_{cspool} = \frac{W_{pool}}{f_{wcovtot}}$$

(62)

when the total amount of water is less than $f_{wcovtot}$ which is a parameter value.

The infiltration capacity at the soil surface is calculated from the saturated conductivity of the topsoil and assuming a unit gradient. During conditions with frost in the soil the saturated conductivity can be reduced because of the ice content in the soil.

A physical barrier for infiltration such as a roof can also be simulated by setting a value larger than zero for the i_{scov} parameter.

Another special feature is the simulation of a furrow similar pattern on the soil surface. In this case only a fraction ($f_{infbypass}$) of the infiltration is going directly to the second compartment of the soil. This means that the furrow receives only ($1 - f_{infbypass}$) of the total infiltration rate originating either from the surface pool or from precipitation.

2.3.6 Lower boundary condition

Different options exist for the lower boundary depending on whether saturated or unsaturated conditions are assumed. If saturated conditions are assumed a ground water outflow as calculated according to the section below will be added to the lower boundary as defined here.

The vertical water flow from the lowest compartment may be calculated by a unit gradient (UNITG = 1) i.e. by gravitational forces only or it may be assumed equal to zero (UNITG=3). Providing that the soil profile is unsaturated (GWFLOW=0) the lower boundary condition may also be defined as a constant soil water tension, ψ_{bottom} (UNITG =0) or a dynamic soil water tension (UNITG=2). If ground water is considered (GWFLOW>=1) the ground water table z_{sat} (UNITG=2) may also be specified as a dynamic variable (DRIVDRAIN ON). Alternatively, if UNITG=4 the flow is calculated as:

$$q_{deep} = \frac{8k_s(z_{sat} - z_{p2})^2}{d_{p2}{}^2}$$

(63)

where k_s is the conductivity of lowest layer, z_{sat} is the simulated depth of the ground water table, z_{p2} is the depth of a drain level with a parallel geometry at a spacing distance of d_{p2}.

2.3.7 Groundwater outflow

Groundwater flow may be considered with different approaches. The different approaches can be combined to account for water flows in different parts of the soil profile depending on the presence of artificial drainage systems and/or topographical and hydrogeological conditions. The groundwater flows are considered as a sink term in the one dimensional structure of the model.

The physically based-approaches can conceptually be compared with a drainage system (see Fig. 16). Water flow to drainage pipes occurs when the simulated groundwater table is above the level of the pipes, i.e., flow occurs horizontally from a layer to drainage pipes when the soil is saturated. In the simplest empirical approach (GWFLOW 1) the horizontal flow rate, q_{wp}, is assumed to be proportional to the hydraulic gradient and to the thickness and saturated hydraulic conductivity of each soil layer:

$$q_{wp} = \int_{z_p}^{z_{sat}} k_s \frac{(z_{sat} - z_p)}{d_u d_p} dz$$ (64)

where d_u is the unit length of the horizontal element, z_p is the depth of the drainage pipe, z_{sat} is the simulated depth of the ground water table and d_p is a characteristic distance. Note that this is a simplification where the actual flow paths and the actual gradients are not represented. Only flows above the drain level z_p are considered.
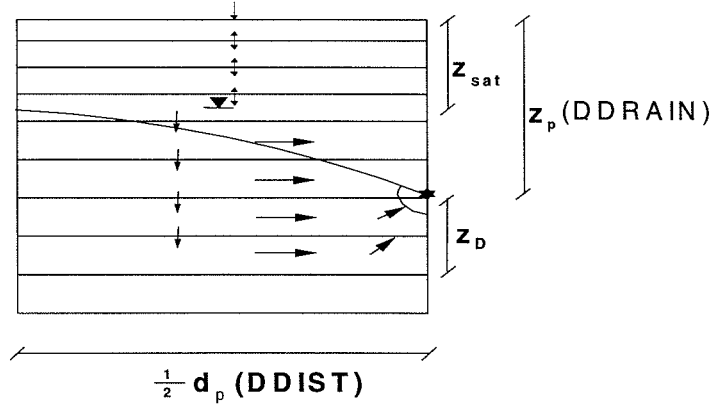
Figure 16. The geometrical assumptions behind the groundwater flow towards a sink point in the saturated zone of the soil. *Den geometriska formen av grundvattenytan mellan två dräneringsrör som är grunden för antagandet om flödet som en sänkterm i modellen.*

A more physically-correct picture of the flow situation may be considered based on of either the classical equations presented by Hooghoudt (1940) and Ernst (1956). Following, Hooghoudt the total flow to pipes is given by:

$$q_{wp} = \frac{4k_{s1}(z_{sat} - z_p)^2}{d_p^2} + \frac{8k_{s2}z_D(z_{sat} - z_p)}{d_p^2}$$ (65)

where k_{s1} and k_{s2} are the saturated conductivities in the horizon above and below drainage pipes respectively, z_D is the thickness of the layer below the drains and d_p is the spacing between parallel drain pipes. In the model, the flows for specific layers above the drain depth are calculated based on the horizontal seepage flow for heterogeneous aquifers (Youngs, 1980) , corresponding to the first term in the Hooghoudt equation:

$$q_{wp1}(z) = \frac{8k_s(z)\left(hu - hl + \frac{(hl^2 - hu^2)}{2(z_{sat} - z_p)}\right)(z_{sat} - z_p)}{d_p^2}$$ (66)

where hu and hl are the heights of the top and bottom of the compartment above the drain level z_p. Below the drain depth the flow is calculated for each layer as:

$$q_{wp2}(z) = \frac{8k_s(z)(z_{sat} - z_p)r_{corr}(z)}{d_p^2}$$ (67)

where the correction factor r_{corr} may be calculated (GWFLOW 5 or 6) based on the equivalent layer thickness (z_d) as:

$$r_{corr}(z) = \frac{z_d \Delta z}{z_D} \qquad (68)$$

where z_d and d_p are related as:

$$\frac{d_p}{z_d} = \frac{\left(d_p - z_D\sqrt{2}\right)^2}{z_D d_p} + \frac{8}{\pi \ln\left(\frac{z_D}{r_p\sqrt{2}}\right)} \qquad (69)$$

where r_p is the diameter of the drain pipe.

Alternatively, the correction factor is based on estimated sums of the radial (r_r), horizontal (r_h) and vertical (r_v) resistances for each layer. The correction factor is then (GWFLOW 3 or 4) given as:

$$r_{corr}(z) = \frac{(r_v(z) + r_h(z) + r_r(z))\Delta z}{r_{href} z_D} \qquad (70)$$

where the r_{href} is the horizontal resistance as included in eq. (67). The separate resistances for each compartment within the z_D layer are given :

$$r_v(z) = \sum_{i=1}^{n} \frac{\Delta z}{k(z)} \qquad (71)$$

$$r_h(z) = \frac{(d_p - \cos(0.5\pi(z_p - z))z_D)^2}{8 K(z) z_D} \qquad (72)$$

$$r_r(z) = \frac{1}{n}\sum_{i=1}^{n} \frac{d_p}{\pi K(z)} \ln \frac{z_D}{r_p} \qquad (73)$$

A return flow (inflow) from the drain pipes or from ditches may be calculated based on straight forward use of the Darcy equation. In this case, the different radial and vertical resistances are neglected and only the horizontal resistance from eq. (64) is applied.

Vertical redistribution within the saturated zone is calculated based on the assumption that the water content will only change in the uppermost saturated layer. Redistribution is calculated such that the losses from all the other layers are satisfied.

One additional empirical approach is based on a first-order recession equation. Unlike the case for the physically-based approach, this sink term will only be calculated in the layer where the ground water table is located and no account is taken of flow paths in the saturated part of the soil profile. When the ground-water level, z_{sat}, is above the bottom of the profile, a net horizontal water flow is given as a sum of 'base flow' and a more rapid 'peak flow':

$$q_{gr} = q_1 \cdot \frac{\max(0, z_1 - z_{sat})}{z_1} + q_2 \frac{\max(0, z_2 - z_{sat})}{z_2} \qquad (74)$$

where q_1, $q2$, z_1, z_2 are parameters obtained by fitting techniques, and z_{sat} is defined as the level where the matric potential is zero.

2.3.8   Groundwater inflow

In a similar way to groundwater outflow (drainage), a horizontal source flow may be defined. The source flow could either be the simulated outflow from a previous simulation (for quasi-two dimensional modelling) or set to a constant value, q_{sof}, for a specific layer, q_{sol}.

In addition, a source flow from a water-filled ditch or stream to the soil profile will be simulated (GWFLOW switch 2, 4 or 6) when the drainage depth is above the groundwater level in the simulated profile.

2.4 Potential transpiration

Transpiration is defined as a potential rate when neither soil water deficits nor low soil temperatures influence the water loss. Unless given directly as a driving variable, daily potential transpiration, TR_p is calculated from Penman's combination equation in the form given by Monteith (1965):

$$L_v TR_p = \frac{\Delta R_n + \rho_a c_p \dfrac{(e_s - e)}{r_a}}{\Delta + \gamma\left(1 + \dfrac{r_s}{r_a}\right)} \qquad (75)$$

where R_n is net radiation available for transpiration (i.e. R_{na} - R_{ns}, see Fig. 20)), e_s is the vapour pressure at saturation, e is the actual vapour pressure, ρ_a is air density, c_p is the specific heat of air at constant pressure, L_v is the latent heat of vaporisation, Δ is the slope of saturated vapour pressure versus temperature curve, γ is the psychrometer 'constant, r_s is an 'effective ' surface resistance. The aerodynamic resistance, r_a, is calculated as:

$$r_a = \frac{\ln^2\left(\dfrac{z_{ref} - d}{z_o}\right)}{k^2 u} \qquad (76)$$

where the wind speed, u, is given at reference height, k is von Karman's 'constant', d is the displacement height and z_o is the roughness length. d And z_o are given explicitly as model parameters.

The roughness length, z_0 is optionally estimated by functions following data presented by Shaw and Periera (1982). Thus:

$$z_0 = \max(h_{canopy}\ \min(f1, f2), z_{0min}) \qquad (77)$$

where f1 and f2 are defined as:

$$f1 = 0.175 - 0.098 p_{densm} + (-0.098 + 0.045 p_{densm})\log(PAI) \qquad (78)$$
$$f2 = 0.150 - 0.025 p_{densm} + (0.122 - 0.0135 p_{densm})\log(PAI)$$

and PAI is the plant area index which is defined as the sum of leaf area index (LAI) and the p_{addind} which is a parameter together with h_{canopy}, p_{densm} and z_{0min}.

Also the displacement height may be estimated by function as derived from the suggestions presented by Shaw and Periera (1982).

$$d = \min(z_{ref} - 0.5,(0.80 + 0.11 p_{densm} - (0.46 - 0.09 p_{densm})e^{-(0.16 + 0.28 p_{densm})PAI} h_{canopy}) \qquad (79)$$

The surface resistance is either considered as a direct function of parameter values (see 0) or it may be calculated as a function of leaf area index (*LAI*), global radiation (R_{ris}) and vapour pressure deficit (e_s -e_a). In the later case the surface resistance is given by:

$$r_s = \frac{1}{\max(LAI\, g_l, 0.001)}$$

(80)

where g_l is the leaf conductance which is given by the Lohammar equation (Lindroth, 199x) as:

$$g_l = \frac{R_{ris}}{R_{ris} + g_{ris}} \frac{g_{max}}{1 + \dfrac{(e_s - e_a)}{g_{vpd}}}$$

(81)

where g_{ris}, g_{max} and g_{vpd} are parameter values.

2.5   Water uptake by roots

Water uptake by roots is assumed to equal actual transpiration, without considering any variations in the water storage of vegetation. Waring et al. (1979) indicated that, for forests, water in vegetation may contribute a considerable amount to transpiration during short periods. Thus, careful interpretation of simulated water uptake rates should be made if within day resolution is considered for a forested site.

Reduction of potential to actual transpiration is performed separately for each depth where the normalized root density, r(z) is above zero. Root density may be expressed by root length per unit soil volume, or by any other pertinent measure of roots.

Reduction because of dry soil is supposed to act through the stomatal mechanism and xylary tissue resistance, which both have shown to be very sensitive to transpiration rate. The water tension response, R_ψ which has been given an analytical form of wide applicability (see Fig. 17.), therefore reacts to the same transpiration demand at all levels:

$$R_\psi(z) = \min\left(\left(\frac{\psi_c}{\psi(z)}\right)^{p_1 TR_p + p_2}, p_3 + \left(\frac{\psi(z)}{\psi_{cw}}\right)(1 - p_3)\right)$$

(82)

where p_1, p_2 and p_3 are parameters as well as the ψ_c and and y_{cw} are a critical tension where reduction begins.
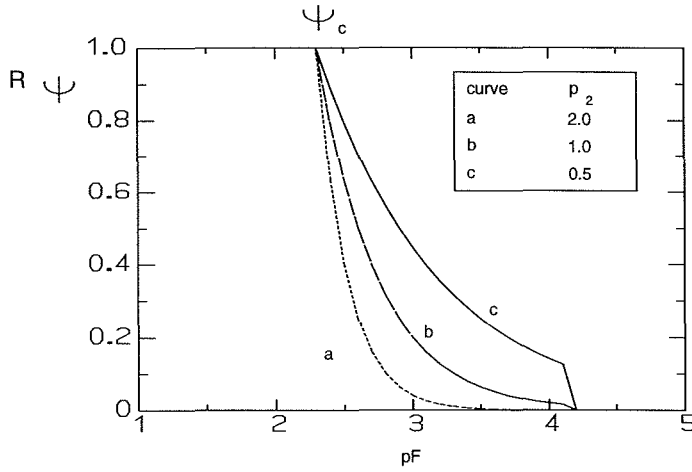
Figure 17. The response of water uptake by roots to soil water tension using different parameter values. *Responsen av markvattentensionen på vattenupptagningen genom rötter.*

curve	p_2
a	2.0
b	1.0
c	0.5

Reduction because of low soil temperatures acts primarily through a lowered conductivity between root surface and xylem and is, thus, responding to temperature at each depth. The analytical form of the soil temperature response (see Fig. 18), R_T, was proposed by Axelsson & Ågren (1976):

$$R_T(z) = 1 - e^{-t_1 \max(0,T(z))^{t_2}}$$

(83)
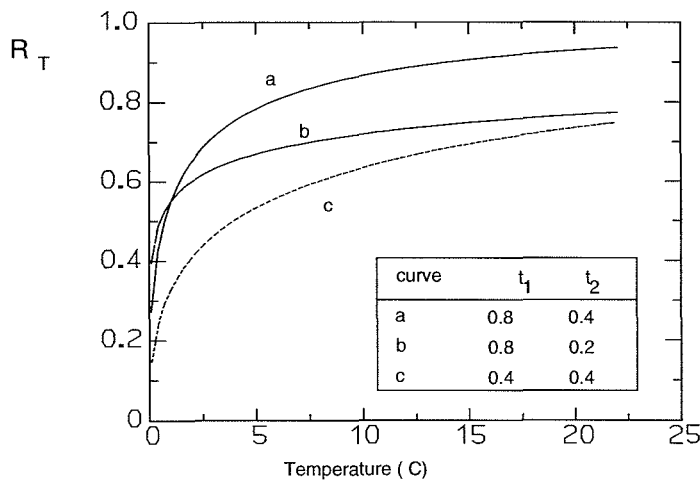
Figure 18. The response of water uptake by roots to soil temperature using different parameter values. Curve (a) corresponds to the default curve suggested by Axelsson & Ågren (1976). *Responsen av marktemperaturen på vattenupptagningen genom rötter. Kurva (a) motsvarar den som föreslogs av Axelsson & Ågren (1976).*

curve	t_1	t_2
a	0.8	0.4
b	0.8	0.2
c	0.4	0.4

Flexibility of a root system to reallocate roots from layers where a deficiency occurs to layers which have an excess of water is accounted for in the model. Actual transpiration is first calculated without any compensatory uptake as:

$$TR_a^* = TR_p^* \int_0^{z_r} R_\psi(z) R_T(z) r(z) dz$$

(84)

where z_r is the maximal root depth. The compensatory uptake is finally accounted for when calculating the total transpiration :

$$TR_a = TR_a^* + f_{umov} \cdot (TR_p^* - TR_a^*)$$

(85)

40

where f_{umov} is the degree of compensation. The compensatory uptake is distributed to the layers where R_ψ is less than unity zero according to the relative fraction of the roots in layers with an excess of water.

2.6 Dynamic behaviour of plant related properties

Some properties which have typical temporal patterns during the season can be varied as a function of the day number t_{day} in the year or they can be given as driving variables in a special file (see "additional driving variable file" in the user's manual) or may be changed step wise by using the switch CHAPAR (see "switches" in the user's manual) . The properties which can be given as functions of time are divided into one group for above ground properties (Surface resistance, r_s, Leaf area index, LAI, Roughness length, z_o , displacement height, d and/or height of canopy and albedo of vegetation) and one for below ground properties (Root depth, z_r). The temporal function is defined by:

$$x = (1 - \alpha)x(i - 1) + \alpha x(i) \tag{86}$$

$$x = x(1) \qquad\qquad\qquad t \le t_{day}(1) \tag{87}$$

$$\alpha = \left(\frac{t - t_{day}(i-1)}{t_{day}(i) - t_{day}(i-1)} \right)^{c_{form}(i-1)} \qquad t_{day}(i-1) < t \le t_{day}(i) \tag{88}$$

$$x = x(i) \qquad\qquad\qquad t > t_{day}(i) \quad \text{and} \quad t_{day}(i+1) = 0 \tag{89}$$

where x (i) is the parameter defined at day number $t_{day}(i)$ in an array from 1 to n. Up to 5 day numbers can be defined, with values > 0 and ≥ 365. If $t_{day}(i)$ is set to 0, only indices lower than i will be considered.
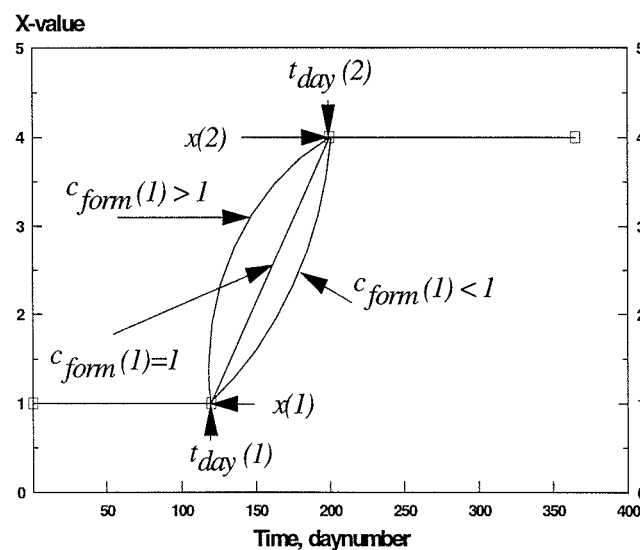
Figure 19. Graphical representation of the interpolation procedure used for some plant related properties according to Eq. (55-58). *Grafisk återgivning av interpolationsförfarandet av växtrelaterade egenskaper enligt ekvationerna (55-58).*

Depth distribution of roots, $r(z)$, can be defined either as a fraction of roots in each horizon according to parameter values or as a functional relationship (uniform, linear or exponential). In a similar way to the uniform and linear function the exponential form is normalized making the integral of the whole soil profile equal to unity. The fraction of roots below a depth z is given by:

$$\int_{z_r}^{z} r(z) = \frac{1 - e^{-k_{rr}(z/z_r)}}{(1 - r_{frac})} \tag{90}$$

where it can be shown that the exponential extinction coefficient k_{rr} equals $- \ln (r_{frac})$. r_{frac} is a parameter in the model.

2.7 ^{K} Evaporation from the soil surface

Soil evaporation can be calculated by two different approaches in the model. The more empirical approach is based on a Penman type equation and the more physically based approach is developed from an iterative solution of the energy balance including both water and heat flow at the soil surface. The empirical approach is normally used when the water balance conditions are of major interest, since it will not influence the soil surface temperature or heat flow. The iterative solution of the energy balance is recommended when the feedback between temperature and water conditions is of interest.

Common to both approaches is the partitioning of net radiation between the plant canopy and the soil surface assuming the Beer's law to be valid (Impens & Lemeur, 1969):

$$R_{ns} = R_{na} e^{-k_{rn}LAI} \tag{91}$$

where R_{na} is the net radiation above the plant canopy, R_{ns} is the net radiation at the soil surface, k_{rn} is an extinction coefficient and LAI is the leaf area index.

The energy flows and resistances in the soil-plant-atmosphere system are illustrated in Fig. 20.
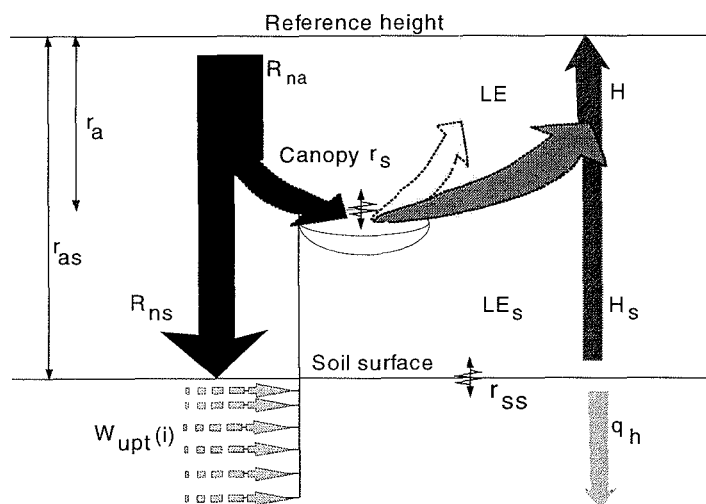
Figure 20 The energy flows and resistances above the canopy and at the soil surface. *Energiflödena och resistanserna ovan kronan och vid markytan.*

---

^{K} water balance; balance, water

2.7.1 [K] Surface energy balance approach

The physically based approach, for calculating soil evaporation, originates from the idea of solving the equation of heat flow at the soil surface boundary. According to the law of conservation of energy:

$$R_{ns} = LE_s + H_s + q_h \qquad (92)$$

where R_{ns} is the available net radiation at the soil surface LE_s is the latent heat flow to the air, H_s is the sensible heat flow to the air and q_h is the heat flow to the soil. The three different heat flows are estimated by an iterative procedure where the soil surface temperature is varied according to a given scheme.

$$H_s = \rho_a c_p \frac{(T_s - T_a)}{r_{as}} \qquad (93)$$

$$LE_s = \frac{\rho_a c_p}{\gamma} \frac{(e_{surf} - e_a)}{r_{as}} \qquad (94)$$

$$q_h = k_h \frac{(T_s - T_1)}{\frac{\Delta z_1}{2}} + Lq_v \qquad (95)$$

where the vapour flow q_v (following eq. 57) from the soil surface to the central point of the uppermost compartment is given by:

$$q_v = d_{vapb} f_a D_0 (T) \frac{c_{vs} - c_{v1}}{\frac{\Delta z}{2}} \qquad (96)$$

where d_{vapb} is the tortuosity given as an empirical parameter, D_0 is the diffusion coefficient for a given temperature, f_a is the fraction of air filled pores. C_{vs} and C_{v1} are the concentrations of water vapour at the soil surface and at the middle of the uppermost compartment respectively.

2.7.1.1 Resistance approach for soil heat flow

As an alternative, the heat flow can be calculated using a simplified resistance approach valid for daily mean values. The flow is then given by:

$$q_h = \frac{T_s - T_1}{r_{soil}} \qquad (97)$$

[K] energy balance; balance, energy

where the r_{soil} represents the integrated resistance of the uppermost 20 cm of the soil profile. The existence of an organic topsoil is accounted for when the resistance is calculated from the thermal conductivity of humus, k_{ho} and of mineral soil, k_{hm}:

$$r_{soil} = \frac{\Delta z_{humus}}{k_{ho}} + \frac{0.2 - \Delta z_{min}}{k_{hm}}$$

(98)

where Δz_{humus} and Δz_{min} are the thickness of humus and mineral soil, respectively in the upper 20 cm of the soil profile.

2.7.1.2 Stability correction and resistance below vegetation canopy

The aerodynamic resistance is influenced by the atmospheric stability through the Richardsons number (R_i) and the crop cover (r_{ab}).

$$r_{as} = \frac{r_a}{\sqrt[3]{(1 - a_{ri} R_i)}} + r_{ab}$$

(99)

where a_{ri} is a parameter with default value 16 taken from to Rosenberg (1978) The Richardsons number is calculated as:

$$R_i = g(h - z_o) \frac{(T_A - T_s)}{(T_A + 273.15)u^2}$$

(100)

where the resistance between the soil surface and the crop canopy, r_{ab}, is made proportional to the leaf area index.

$$r_{ab} = r_{alai} LAI$$

(101)

where r_{alai} is a parameter

2.7.1.3 Moisture availability at the soil surface

Vapour pressure at the soil surface is given by the surface temperature, T_s, the water tension of the uppermost layer and an empirical correction factor, e_{corr}, accounting for steep gradients in moisture between the uppermost layer and the soil surface.

$$e_{surf} = e_s(T_s) e^{\left(\frac{\frac{-\psi}{100} M g e_{corr}}{R(T_s + 273.15)} \right)}$$

(102)

where R is the gas constant, M is the molar mass of water and g is the gravity constant..

The empirical correction factor depends on a parameter ψ_{eg} and a calculated mass balance at the soil surface, δ_{surf}, which is allowed to vary between the parameters s_{def} and s_{excess} given as mm of water.

$$e_{corr} = 10^{(-\delta_{surf}\psi_{eg})} \tag{103}$$

$$\delta_{surf}(t) = \max(s_{def}, \min(s_{excess}, \delta_{surf}(t-1) + (I - E_s - q_v)\Delta t) \tag{104}$$

where I is the infiltration rate, E_s is the evaporation rate and q_v is the vapour flow from soil surface to the central point of the uppermost soil layer.

2.7.2 Empirical approach for soil evaporation

The radiation energy reaching the soil surface, R_{ns}, is used to calculate the soil surface evaporation, E_s using the Penman combination equation:

$$LE_s = \frac{\Delta(R_{ns} - q_h) + \rho_a c_p \dfrac{(e_s - e)}{r_{as}}}{\Delta + \gamma\left(1 + \dfrac{r_{ss}}{r_{as}}\right)} \tag{105}$$

where r_{as}, is the sum of the aerodynamic resistance and r_{ss} is the surface resistance at the soil surface.

The aerodynamic resistance between the soil surface and the reference height, r_{as}, is calculated in the same way as in the physically based approach using Eq. (82).

The surface resistance at the soil surface, r_{ss} can be given by two alternative empirical functions accounting for moisture conditions at the soil surface and the water tension in the uppermost soil layer, either:

$$\begin{aligned} r_{ss} &= r_\psi(\log\psi - 1 - \delta_{surf}) & \psi &> 100 \\ r_{ss} &= r_\psi(1 - \delta_{surf}) & \psi &< 100 \end{aligned} \tag{106}$$

or

$$r_{ss} = \max(0, r_{\psi 1} \max(\psi - r_{\psi 2}, 0) - r_{\psi 3}\delta_{surf}) \tag{107}$$

where r_ψ is an empirical coefficient and ψ is the water tension in the uppermost layer. As above, δ_{surf} is the mass balance at the soil surface, in units of mm water, which is allowed to vary between s_{def} and s_{excess}. The mass balance at the surface is calculated by Eq. (94) as in the energy balance approach. The soil surface temperature will also be estimated if the switch

---

^K mass balance; balance, mass

SUREBAL is put to the value 1. This is done by first solving the heat balance equation for the sensible heat flow to the air as:

$$H_s = R_{ns} - LE_s - q_h$$
(108)

where the soil heat flow, q_h, is taken as an weighted sum of the heat flow from the preceding time steps. The soil surface temperature is finally given as:

$$T_s = \frac{H_s r_{as}}{\rho_a c_p} + T_a$$
(109)

2.8 Evaporation of intercepted water

A simple threshold formulation gives the interception rate of precipitation, S_{int}, by the vegetation canopy:

$$S_{int} = \min\left(P, \frac{(S_{i\max} - S_i(t-1))}{\Delta t} \right)$$
(110)

where P is precipitation, S_{imax} is the interception storage threshold, and S_i $(t-1)$ is the interception storage remaining from the previous time step. S_{imax} is a function of the leaf area index, LAI:

$$S_{i\max} = i_{LAI} LAI$$
(111)

where i_{LAI} is a parameter.

Infiltration to the soil, $q_w(0)$ is then:

$$q_w(0) = \max(0, P - S_{int})$$
(112)

In forests, evaporation of intercepted water may considerably exceed transpiration rates with equivalent local-climatic conditions.

The potential evaporation rate, EI_p, from interception storage can either be calculated from the Penman combination equation assuming a surface resistance (r_{sint}) representing the resistance to the single source point of the whole canopy. When potential transpiration is used as a driving variable a constant relation between wet surface evaporation rate and potential transpiration rate is assumed:

$$EI_p = e_{rat} TR_p$$
(113)

46

where e_{rat} is a parameter. If the Penman combination equation is used to calculate EI_p, the e_{rat} value is given by the equation above and not taken as a parameter.

Actual evaporation from the canopy is limited either by the potential daily rate, EI_p, or by the interception storage, S_{int}:

$$EI_a = \min\left(EI_p, S_{int} + \frac{S_i(t-1)}{\Delta t} \right) \tag{114}$$

where $S_i(t-1)$ is the residual intercepted water which remains from the previous time step (Δt) if the actual evaporation, EI_a, was smaller than the interception storage. Remaining intercepted water at the present time step is calculated as:

$$S_i(t) = S_i(t-1) + (S_{int} - EI_a)\Delta t \tag{115}$$

When evaporation of intercepted water, EI_a, takes place the potential transpiration rate, TR_p is reduced based on the assumption that evaporation and transpiration are complementary in time:

$$TR_p^* = \max\left(0, TR_p - \frac{EI_a}{e_{rat}} \right) \tag{116}$$

Evapotranspiration, i.e., the total water loss to the atmosphere per unit ground surface, is calculated as the sum of actual transpiration and wet surface evaporation. This yields the final expression for daily evapotranspiration, ET:

$$ET = EI_a + E_s + TR_a \tag{117}$$

2.9 Snow Dynamics
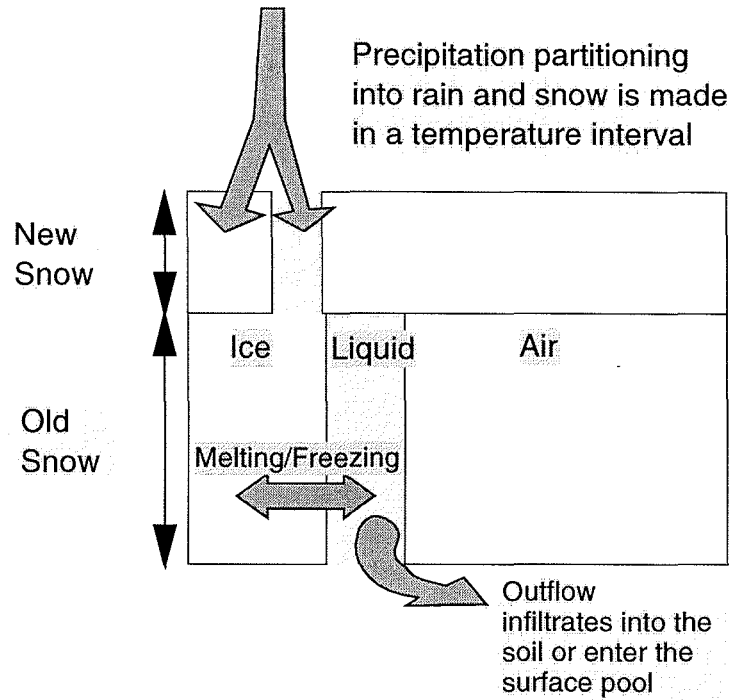
Figure 21 The snow model, subdivision of snow into two compartments and the different water flow paths. Snörutinen med uppdelning av snön i två skikt och med de olika vattenflöden som beräknas i modellen.

Snow is separated into liquid water and the total water equivalent. The entire snow pack is considered to be homogeneous both horizontally and vertically and only day to day variations are calculated. The fundamental part of the model is the melting-freezing function which combines the two separate budgets. Daily amount of snow melt, M, is made up by a temperature function, M_T, a function accounting for influence of solar radiation, M_R, and the soil surface heat flow, q_h (0):

$$M = M_T T_a + M_R R_{is} + \frac{f_{qn} q_h(0)}{L_f}$$

(118)

where T_a is air temperature and R_{is} is global radiation. Melting will affect the whole snow pack, whereas refreezing will only affect a limited surface layer. Refreezing efficiency is, therefore, inversely proportional to snow depth, Δz_{snow}:

$$M_T = m_T \qquad\qquad\qquad T_a \geq 0$$

$$M_T = m_T \min\left(1, \frac{m_f}{\Delta z_{snow}}\right) \qquad T_a < 0$$

(119)

where T_a is air temperature and m_T And m_f are parameters.

Albedo is markedly reduced with age of snow surface, such that radiation absorption increases with time. This is the reason for making M_R dependent on the age of the surface snow, t_{sage}:

$$M_R = m_{R\min}(1 + s_1(1 - e^{-s_2 t_{sage}}))$$

(120)

where m_{Rmin}, s_1 and s_2 are parameters. Age of surface snow is determined by the number of days since the last snowfall. To reduce the influence of mixed precipitation and minor showers, snowfall is counted in this context only for snow spells larger than a critical value, P_{samin}, and for precipitation with thermal quality above a threshold value Q_{samin}.

The accumulation of free water in the snow pack is calculated on a daily basis as:

$$S_{wl} = S_{wlres} + P_r + M$$

(121)

where S_{wlres} is the free water remaining from the previous day, P_r is the rain precipitation, and S is the water equivalent (total amount of water in the snow pack) and with the restriction that $0 < S_{wl} < S$. If the free water is above a given retention threshold, S_{wlmax}, it will be released as infiltration:

$$q_w(0) = \max(0, S_{wl} - S_{wl\max})$$

(122)

such that the remaining amount of free water becomes:

$$S_{wlres} = s_{wl} - q_w(0)$$

(123)

The retention capacity is assumed to be a fixed fraction, f_{ret}, of the snow pack water equivalent:

$$S_{wl\max} = f_{ret}S$$

(124)

The snow pack not only contributes melt water to infiltration but soil surface temperature is also influenced through snow depth and thermal conductivity (cf. Eqs. 7 and 8).

Snow thermal conductivity, k_{snow} is sensitively related to snow density, ρ_{snow} (Corps of Engineers, 1956):

$$k_{snow} = s_k \rho^2_{snow}$$

(125)

where s_k is an empirical parameter, and snow density is a weighted average of the old snow pack (i.e. the density of snow remaining from the previous day ρ_{old}) and precipitation density, ρ_{prec}:

$$\rho_{snow} = \frac{\rho_{prec}\Delta z_{prec} + \rho_{old}\Delta_{old}}{\Delta z_{snow}}$$

(126)

where Δz indicates depth and the indices represent old snow pack, precipitation and updated snow pack.

A perfectly frozen precipitation is assumed to have a constant, minimum density, ρ_{smin}. For mixed precipitation, density depends on the ratio of rain, P_r, to total precipitation, P:

$$\rho_{prec} = \rho_{s\min} + (\rho_{water} - \rho_{s\min})\frac{P_r}{P} \qquad (127)$$

Depth of precipitation is then automatically given as:

$$\Delta z_{prec} = \frac{P}{\rho_{prec}} \qquad (128)$$

Density of the old snow pack increases with the relative amount of free water in the pack and with overburden pressure, i.e., with increasing water equivalent. Density also generally increases with age. The age dependency is accounted for by updating density as the maximum of the previous day's density or:

$$\rho_{old} = \rho_{s\min} + s_{dl}\frac{S_{wl}}{S_{wi\max}} + s_{dw}S_{res} \qquad (129)$$

where s_{dl} and s_{dw} are parameters and S_{res} is the water equivalent of the snow pack from the previous day. Depth of old pack is given by definition as:

$$\Delta z_{old} = \frac{S_{res}}{\rho_{old}} \qquad (130)$$

50

3.   Model input

Three classes of input data may be distinguished. Driving variables are the climatic data which govern the model. Initial values are required to define a starting point at a specific time and physical parameters are constants needed to express relevant properties for the different processes in the model. However, some of these properties may be varied with time and this could either be done by using time dependent functions for some of the parameters or by selecting a new value of a certain parameter to be valid at a specified date (see Switches CHAPAR).

3.1   Driving variables

The SOIL model can be run in several simulation modes depending on the purpose of the simulation. Each mode has its own requirements for driving variables. If, for example, soil temperature is simulated with variations within the day and with soil moisture treated as constant, a measured top soil temperature will suffice as a single driving variable. If the aim is to simulate effects of soil heat extraction on an annual basis, air temperature, precipitation and heat extraction rate will suffice as measured driving variables, since in this case potential transpiration can be given as a simplified analytical function to account for annual variations.

The most common simulation mode, thus far, has been to simulate, on an annual basis, both soil heat and water flows in a natural, vegetated soil. This mode requires the input of the following meteorological variables once a day: Precipitation, air temperature, relative humidity, wind speed, net radiation and global, shortwave radiation. Ideally, these variables should be measured at a reference height above vegetation, but being daily sums or averages, it will commonly be sufficient to use data from a nearby standard meteorological network station. If, by chance, a reliable measure of potential transpiration can be given, this measure will substitute relative humidity, wind speed and net radiation. If, on the other hand, some of the driving variables are not measured, they can be substituted by analytical expressions or they can be deduced from other measurements. Global radiation can be substituted by degree of cloudiness or duration of bright sunshine. Relative humidity, wind speed and cloudiness could each be substituted by parameter values representing average conditions for longer time periods. Net radiation can be substituted by global radiation. The minimum requirement to produce realistic results from simulations of annual heat and water flows is to have only measured precipitation and air temperature.

In the present form, treatment of driving variables and simulation mode options mainly reflect past development and use of the model but new options can easily be included, if needed for a specific purpose.

Potential transpiration is normally calculated in the model by Monteith's equation (Eq. 48) in which case account is also made for heat flow into the soil. Potential transpiration can also be given directly as a measured time series or as an analytical expression:

$$TR_p = 0 \qquad\qquad \left| t - t_{p\max} \right| \ge \Delta t_T$$

$$TR_p = TR_{p\max} \sin\left(\left(\frac{(t - t_{p\max} + \Delta t_T)}{2\Delta t_T}\right)\pi\right) \qquad\qquad (131)$$

$$\left| t - t_{p\max} \right| < \Delta t_T$$

This function gives a "smooth pulse" with a half width of Δt_T and a maximal value of $TR_{p\max}$ at time t_{pmax}.

51

Precipitation can be given as a series of pulses, with regular frequency and specified pulse height. Normally, however, it is given as a measured time-series. To account for the precipitation phase, i.e., whether snow or rain, thermal quality, Q, i.e., relative fraction of frozen water, is calculated from air temperature, T_a:

$$Q = 0 \qquad\qquad\qquad T_a > T_{max}$$
$$Q = \frac{(T_a - T_{max})}{(T_{min} - T_{max})} \qquad T_{min} \leq T_a \leq T_{max} \qquad (132)$$
$$Q = 1 \qquad\qquad\qquad T_a < T_{min}$$

Where all precipitation is assumed to be rain for air temperatures above T_{max} and to be snow for air temperatures below T_{min}. Between these limits proportions vary linearly. Rain, P_r, and snowfall, P_s, is, thus, given from precipitation as:

$$P_r = (1 - Q)P \qquad\qquad\qquad\qquad (133)$$
$$P_s = QP \qquad\qquad\qquad\qquad\qquad (134)$$

Measured precipitation, P_m, is almost always less than the "true" value, P, primarily because of wind-losses. These losses are more pronounced for snowfall than for rain. An acceptable long-term, average, correction can be given by multiplying the measured value by a constant fraction, different for rain and snowfall:

$$P = (c_{rain} + Qc_{snow})P_m \qquad\qquad\qquad (135)$$

For Swedish conditions, the Swedish Meteorological and Hydrological Institute (SMHI) recommends a rain correction of 7% and a snow correction of 15%, meaning that $c_{rain} = 1.07$ and $c_{snow} = 0.08$.

Air temperature is normally supplied as a measured value, sometimes being the average of a night- and a day-time temperature. It can also be given an analytical form:

$$T_a = T_{amean} - T_{aamp}\cos\left(\frac{t - t_{ph}}{y_{cycle}}2\pi\right) \qquad\qquad (136)$$

which, with correct choices of parameters T_{amean}, T_{aamp}, t_{ph} and y_{cycle}, can properly represent both diurnal and annual variations.

Topsoil temperature, when used as a driving variable, is supplied as a measured time-series.

The air humidity can either be expressed as relative humidity, h_r, or as the actual vapour pressure (e). *The air humidity*, is normally supplied as a measured time-series but if it is not available a constant value of the relative humidity can be specified as a parameter. The vapour pressure, e_a, will be calculated from air temperature if the relative humidity is used and from the vapour pressure, e_a, the vapour pressure deficit, δe, is calculated:

$$e_a = \frac{h_r}{100} e_s(T_a)$$
(137)

$$\delta e = e_s(T_a) - e_a$$
(138)

The saturated vapour pressure function, $e_s(T)$, is defined by:

$$e_s(T) = 10^{\left(12.5553 - \frac{2667}{T+273.15}\right)}$$ $T \geq 0$ (139)

$$e_s(T) = 10^{\left(11.4051 - \frac{2353}{T+273.15}\right)}$$ $T < 0$ (140)

where e_s is calculated in (Pa) and T in °C.

Wind speed is normally supplied as a measured time-series but it can be substituted by a constant parameter value if it is not available. Wind speeds less than 0.1 mm/s are rejected and replaced by this lower limit.

Net radiation would ideally be supplied as a measured time-series but in most cases it has been estimated from other meteorological variables. It can be deduced from global radiation, R_{is}, air temperature, T_a, vapour pressure, e_a, and relative duration of sunshine, n_{sun}, as the sum of net shortwave, R_{ns}, and net loss of longwave radiation, R_{nl}, the latter given by Brunt's formula:

$$R_n = R_{nsh} - R_{nl}$$
(141)

where

$$R_{nsh} = R_{is}(1 - \alpha_r)$$
(142)

and

$$R_{nl} = 86400\sigma(T_a + 273.15)^4 (r_1 - r_2\sqrt{e})(r_3 + r_4 n_{sun})$$
(143)

where α_r is shortwave r_1 to r_4 are empirical parameters and σ is Stefan-Boltzmann's constant.

As an alternative formula for the net long wave radiation the user may also chose:

$$R_{nl} = 86400\sigma((T_S + 273.15)^4 - (rr_1 - rr_2\sqrt{e})(T_a + 273.15)^4)(rr_3 + rr_4 n_{sun})$$
(144)

where the temperature of the soil surface T_s is explicitly used.

The albedo value will be calculated as a function of the albedo for vegetation and the albedo of the soil surface as:

$$a_r = a_{soil} e^{(-LAI\,k_{rn})} + (1 - e^{(-LAI\,k_{rn})})a_{veg}$$
(145)

where a_{veg} is given as parameter values similar to other vegetation characteristics (see 0) .The k_{rn} is the same parameter as used for extinction of net radiation and a_{soil} is calculated as:

$$a_{soil} = a_{dry} + e^{-k_a{}^{10}\log(\psi)}(a_{wet} - a_{dry})$$

(146)

where k_a is parameter as well as the albedo for a dry (a_{dry}) and wet soil (a_{wet}) respectivily. The soil water tension of the uppermost layer (ψ_l) is allowed to vary from 10^1 to 10^7 cm

Relative cloudiness, : n_c, can be used to calculate relative duration of sunshine, n_{sun}:

$$n_{sun} = 1 - n_c$$

(147)

Duration of bright sunshine, Δt_{sun}, can also be used to estimate relative duration of sunshine:

$$n_{sun} = \frac{\Delta t_{sun}}{\Delta t_{max}}$$

(148)

Daylength, Δt_{max}, is calculated as a function of the latitude:

$$\Delta t_{max} = 1440. - \frac{120}{rad \cdot 15} \arccos(a_1)$$

(149)

where rad is a radian and the argument in the arc cosines function a_1 is given as:

$$a_1 = \min(1, \max(-1, \frac{\sin(rad \cdot lat) \cdot \sin(rad \cdot dec)}{\cos(rad \cdot lat) \cdot \cos(rad \cdot dec)}$$

(150)

where the declination dec is given as:

$$dec = -23.45 \cos\left(3.14 \frac{(t_{day} + 10.173)}{182.61}\right)$$

(151)

Global shortwave radiation is normally supplied as a measured time-series. If not directly measured, it can be deduced from potential global radiation, R_{pris}, and relative duration of sunshine, n_{sun}, with Ångström's formula:

$$R_{is} = R_{pris}(r_5 + r_6 n_{sun})$$

(152)

where r_5 and r_6 are turbidity constants.

Potential global radiation above the atmosphere is given as a function of the declination, dec, and daylength, Δt_{max}:

$$R_{pris} = 1360 \cdot 60 \cdot a_2 \cdot \Delta t_{max}$$

(153)

54

where daylength, Δt_{max} is given by Eq. (139) and

$$a_2 = \sin(rad \cdot lat) \cdot \sin(rad \cdot dec)$$ (154)

$$-\frac{\cos(rad \cdot lat) \cdot \cos(rad \cdot dec)}{\Delta t_{max} / 120 \cdot rad \cdot 15} \sin\left(rad \cdot 15\left(24 - \frac{\Delta t_{max}}{120}\right)\right)$$

where the declination *dec* is given by Eq. (141).

Two man-made climatic impacts can also be considered:

Irrigation can be given as a measured time-series or specified to take place at certain soil moisture conditions. The irrigation is considered either as totally above vegetation ($i_{sfrac} = 0$), totally at the soil surface ($i_{sfrac} = 1$) or with any other partition ($0 < i_{sfrac} < 1$) between the vegetation and the soil.

The control of irrigation is governed by the actual soil water storage S_{swat} which is the sum of water storage in a number of layers (n_{isl}). When S_{swat} drops below a critical threshold S_{smin} irrigation of an amount i_{am} takes place at an intensity i_{ar}.

Soil heat extraction rate from a specified layer, z_{nhp}, can be given as a measured time-series but may also be given as a function of air temperature according to governing rules for commercially available soil heat pump equipment:

$$s_h = s_{h1}$$ $$T_a < T_{hpc}$$ (155)

$$T_a \geq T_{hpc}$$ (156)

$$s_h = \min(s_{hp\,max}, s_{h1} + s_{h2}(T_{hp\,lim} - T_a))$$

where s_{h1} is a constant heat extraction required for hot water purposes, T_{hpc} a critical temperature below which domestic heating is necessary and s_{h2} And T_{hplim} are design parameters in the air temperature dependence.

When the soil temperature drops below T_{hpcut} the extraction rate will be reduced according to

$$s_h = 0$$ $$T_s \leq T_{hp0}$$

$$s_h = s_h \cdot \frac{T_s - T_{hp0}}{T_{hpcut} - T_{hp0}}$$ $$T_s \geq T_{hp0}$$ (157)

where T_{hp0} is the temperature at which the heat extraction reaches ceases.

3.2 Initial values

Initial values are needed for all state variables in the model, i.e., snow water equivalent, snow thermal quality, interception water storage, heat and water contents in each of the soil compartments.

Initial soil water contents may be specified as a (measured) profile or as a constant value for the whole profile. Initial water contents may also be deduced from a soil water potential profile or

from a constant, i.e., equilibrium potential in the whole profile. If a ground water table exists above the lower boundary it should be separately assigned a starting value.

Initial soil heat contents are commonly given directly only in combination with the INSTATE option when several consecutive simulations must be started with the same initial values, specified only once before the first simulation. Heat contents are complex functions of solid soil properties, soil freezing, soil water content, compartment thickness and soil temperature. Thus initial soil temperatures are instead normally used to specify initial heat content values. Initial temperatures can be given either as a single value or as a (measured) profile. When heat content is calculated from temperature in partially frozen conditions, the same solution is used as in Eq. (26).

3.3 Physical parameters

Different types of parameters are found in the computer program. Option parameters are used to choose between different simulation modes etc. Initial value parameters have no meaning except to provide a starting point for the simulation. Parameters defining soil compartment thickness are important when concerning numerical stability. Physical parameters, as defined in this section, refer only to those parameters (i.e. constant) which are intrinsic components of process equations.

The number and type of physical parameters are good measures of the degree to which a model rests on basic physical foundations. An attempt has been made in Table 1 to classify the physical parameters in the SOIL model according to present model applications. Class A refers to those parameters whose values are well established, whereas class B refers to parameters whose values rest on more subjective grounds. A_1 parameter values have been measured directly with surmountable effort. A_2 parameters have values taken from established knowledge. B_1 parameter values have been optimized from time-series of the entity to be predicted by the model, whereas B_2 parameter values are more or less safe 'guesstimates', based as far as possible on the best existing knowledge. Division of parameters into the various process categories is somewhat arbitrary, and it should be clear that several parameters directly influence more than one process.

Ideally all parameters should be of type A, but in some cases this will not even be theoretically possible. This is the case, for instance, for groundwater parameters. Since groundwater movements are governed by forces outside the system, groundwater should in a strict sense be regarded as a driving variable. When present in the model, it is, however, possible to predict groundwater movements with reasonable accuracy, provided there is a sufficiently long time-series for estimation.

The number of model parameters depend on the degree to which driving variable processes have been included. If, for instance, net radiation is measured, there will be no need to include albedo in the model. On the other hand, it is a rather subjective choice not to include Brunt's coefficients (cf. Eq. 110) as model parameters when net radiation is calculated from other available climatic data. It is also a rather subjective choice when parameters are not explicitly expressed in the programme, simply implying their values to unity or zero, or to a fixed numerical value. This is done, for instance, when putting density of mineral soil solids to 2.65 g/cm, thereby implying a unique relationship between dry bulk density and porosity.

It is not meaningful to discuss generally the sensitivity of a model to variations in parameter values, but from present applications of the SOIL model, a few parameters have always been found to be of importance. Surface resistance and interception threshold represent the major controls of water loss to the atmosphere. Soil heat balance is strongly affected by depth of the humus layer, and on an annual basis, both heat and water balances depend sensitively on snow melt which is primarily determined by the two constants relating melting to air temperature and global radiation. The parameter values which are most difficult to determine accurately for soil

water calculations, are the saturated conductivity and parameters that controls the unsaturated conductivity (e.g. the tortuosity factor).

Table 1. Physical parameters for the various parts of the SOIL model. Parameter derivations is A: directly measured (1) or established knowledge (2), or B: estimated by fitting techniques (1) or 'guesstimates' (2) *Fysikaliskt baserade parameterar för olika delar av modellen. Där kategori A uppdelas i direkt mätta (1) eller känd kunskap (2) och kategori B uppdelas i (1) skattade genom anpassning eller (2) genom intelligenta gissningar*

Group	Parameter	Definition	Parameter derivation			
			A_1	A_2	B_1	B_2
Driving variables	c_{rain}	Wind correction, rain		x		
	c_{snow}	Wind correction, snow		x		
Soil properties	a_{scale}	Aggregates, scaling			x	
	λ	Pore size distribution	x			
	θ_r	Residual water content	x			
	θ_m	Water content for macropores	x			
	θ_s	Porosity	x			
	θ_w	Water content at wilting point	x			
	Ψ_a	Air entry pressure	x			
	k_{sat}	Saturated conductivity, including macropores	x			
	k_{mat}	Saturated conductivity, excluding macropores		x		
	k_{minuc}	Minimum conductivity		x		
	a, gn, gm	Van Genucheten coefficients	x			
	n	Tortuosity factor		x		
	Ψ_x	Upper limit for use of the Brooks & Corey expression	x			
	$p_{hysmaxc}$	Maximal hysteresis on conductivity function				x
	p_{hysmax}	Maximal hysteresis on water retention				x

Group	Parameter	Definition	Parameter derivation			
			A_1	A_2	B_1	B_2
	a_{PF1}	Lower threshold in shift point function				x
	a_{PF2}	Upper threshold in shift point function				x
	$a_{\theta d}$	Range for obtaining hysteresis during sorption				x
	$a_{\theta D}$	Threshold rate to obtain hysteresis during sorption				x
	a_{hysk}	Age response coefficient				x
	a_{1-3}	Thermal conductivity, Kerstens equation, unfrozen soil		x		
	b_{1-4}	Thermal conductivity, Kerstens equation, frozen soil		x		
	h_{1-2}	Thermal conductivity, Organic soil		x		
	Δz_{humus}	Thickness of humus layer		x		
	$q_h(low)$	Geothermal heat flow	x			
	d_1	Unfrozen water content coefficient		x		
	d_2	Freezing point depression		x		
	d_3	Freezing point depression		x		
	fc_i	Impedance parameter for the effect of ice on hydraulic conductivity		x		
Evapotrans-piration	α_r	Albedo for vegetation and soil	x			
	α_{veg}	Albedo for vegetation	x			
	α_{dry}	Albedo for dry soil	x			

Group	Parameter	Definition	A_1	A_2	B_1	B_2
	α_{wet}	Albedo for wet soil	x			
	d	Displacement height		x		
	z_0	Roughness length		x		
	r_s	Surface resistance			x	
	e_{rat}	Evaporation ratio			x	
	i_{LAI}	Specific interception capacity		x		
	r_{sint}	Surface resistance		x		
	LAI	Leaf area index	x			
Soil evaporation	ψ_{eg}	Surface vapour pressure dependence				x
	r_{alai}	Aerodynamic resistance				x
	a_{ri}	stability coefficient		x		
	r_ψ	Coefficient in soil surface resistance				x
	$r_{\psi 1}$	Coefficient in soil surface resistance				x
	$r_{\psi 2}$	Coefficient in soil surface resistance				x
	$r_{\psi 3}$	Coefficient in soil surface resistance				x
	k_{rn}	Extinction coefficient		x		
	s_{def}	Maximal deficiency at soil surface				x
	s_{excess}	Maximal excess at soil surface				x
Root water uptake	ψ_c	Critical soil water tension		x		
	p_1	Water tension function		x		
	p_2	Water tension function		x		
	t_1	Temperature function		x		
	t_2	Temperature function		x		
	f_{umov}	Compensatory uptake				x
	r_{frac}	Exponential root function			x	
		Root fraction			x	
	z_r	Root depth			x	
		Daynumber for Root			x	

Group	Parameter	Definition	A_1	A_2	B_1	B_2
		depth				
Ground water	z_1	Ground water depth			x	
	z_2	Ground water depth			x	
	q_1	Ground water flow			x	
	q_2	Ground water flow			x	
	d_p	Characteristic distance		x		
	z_p	Depth of drain pipes		x		
		Layer for source flow		x		
		Rate of source flow		x		
	w_{pmax}	Maximal amount of water stored on the surface without causing surface runoff			x	
	$f_{wcovtot}$	Amount of water on the soil surface when entire area is covered			x	
	$f_{infbyfrac}$	Fraction bypassing to second layer				x
	a_{surf}	Surface runoff coefficient			x	
Snow	T_{max}	Rain threshold		x		
	T_{min}	Snow threshold		x		
	S_1	Age coefficient				x
	S_2	Age coefficient				x
	P_{samin}	Age coefficient				x
	Q_{samin}	Age coefficient				x
	s_{dl}	Snow density				x
	s_{dw}	Snow density				x
	ρ_{smin}	Snow density				x
	s_{wlmin}	Liquid water threshold				x
	m_f	Refreezing				x
	m_{Rmin}	Melting coefficient				x
	m_T	Melting coefficient				x
	f_{ret}	Retention capacity				x
	s_k	Thermal conductivity				x

4. Numerical computation

The two partial differential equations (2) and (32) are solved with an explicit forward difference method (Euler integration). This solution requires the soil profile to be approximated with a discrete number of internally homogeneous layers.

Slowly changing state variables are bypassed and changes of the integration time step are made during simulation to speed up execution times.

4.1 Soil Compartmentalization

The soil profile (Fig. 7) is divided into a number of compartments (maximum 22) with arbitrary thickness. Compartment thicknesses are the same for state variables of both heat and water.

To ensure conditions at the lower boundary the soil profile should normally be deep enough to make vertical soil heat flow close to zero. To simulate variation of heat flow within the day, for one week, a profile depth of about one metre is normally required. If the annual cycle is to be simulated, profile depth must extend to between 10 and 20 m, depending on soil type. Site specific groundwater conditions also influence the necessary depth. A minimum soil depth must include the root zone and the underlying unsaturated zone where capillary rise can occur. This depth, however, is normally well above the depth required to obtain a well defined lower boundary condition to the heat flow equation.

The chosen thickness of individual compartments depend on temporal extent and resolution of the simulation. The thickness of compartments are chosen to account for the morphological structure of the soil and numerical requirements of the solution method. Since both variation in vertical soil properties and temporal variations of state variables are most pronounced near the soil surface the smallest compartments are needed there. A compartment thickness of not more than 2 cm is needed to simulate variation within the day. If only annual resolution is required the smallest compartment can be extended to about 10 cm thereby decreasing the necessary execution time by a factor of 25 compared to the solution with the 2 cm compartment.

4.1.1 Difference approximation of soil heat and water flow equations.

To calculate the flow between two adjacent compartments, a finite difference approximation is made. The governing gradients of temperature (Eq. 1) and total water potential (Eq. 31) are calculated linearly between the mid-points of consecutive compartments. The flow is given by:

$$q_{i,i+1} = k_{i,i+1}(\theta_{i,i+1}) \frac{\phi_i - \phi_{i+1}}{\dfrac{\Delta z_i + \Delta z_{i+1}}{2}}$$

(158)

where i designates the layer number, Φ the appropriate potential and Δz the layer thickness

In case of the water flow the total potential is the sum of both matric potential and the gravity potential. The gravity potential is directed from the soil surface downwards which justify the use of a single ended approximation of the inter-block conductivity between compartments. Thus the water flow may be given as:

$$q_{i,i+1} = k_{i,i+1}(\theta_{i,i+1}) \frac{\psi_i - \psi_{i+1}}{\dfrac{\Delta z_i + \Delta z_{i+1}}{2}} + k_{i,i+1}(\theta_i)$$

(159)

The numerical solution is sensitive to the choice of inter-block conductivity (Haverkamp & Vauclin, 1979). A number of different methods to obtain this inter-block conductivity were discussed by Halldin et al. (1977). The solution used by the SOIL model is obtained by defining conductivity at the boundary between two bordering compartments. States, and parameters defining conductivities, are assumed to vary linearly between mid-points of compartments. Water content at the boundary between two compartments is, thus, given by:

$$\theta_{i,i+1} = \frac{\Delta z_i \theta_{i+1} + \Delta z_{i+1} \theta_i}{\Delta z_i + \Delta z_{i+1}}$$ (160)

The only exception to this procedure is the gravity generated flow of water which is using the water content of the upper compartment instead of the boundary water content.

4.1.2 Compartmentalization of soil properties

Soil heat and water characteristics must be defined for each compartment and thermal and unsaturated conductivity's must be defined for each boundary between compartments in the soil profile. Available field data representing these properties seldom coincide exactly with the chosen discretization of the soil profile.

Continuous profiles of soil properties are obtained by linear interpolation between, and extrapolation outside of measurement or sampling depths (Fig. 21). From a continuous profile of a parameter, p (z), discrete parameter values are obtained for each compartment by:

$$p_i = \int_{z_i}^{z_{i+1}} \frac{p(z)dz}{(z_{i+1} - z_i)}$$ (161)

where : z_i and z_{i+1} are the upper and lower boundaries of compartment i. Conductivity parameters are calculated for each boundary between compartments by:

$$p_{i,i+1} = \frac{\Delta z_i p_{i+1} + \Delta z_{i+1} p_i}{\Delta z_i + \Delta z_{i+1}}$$ (162)
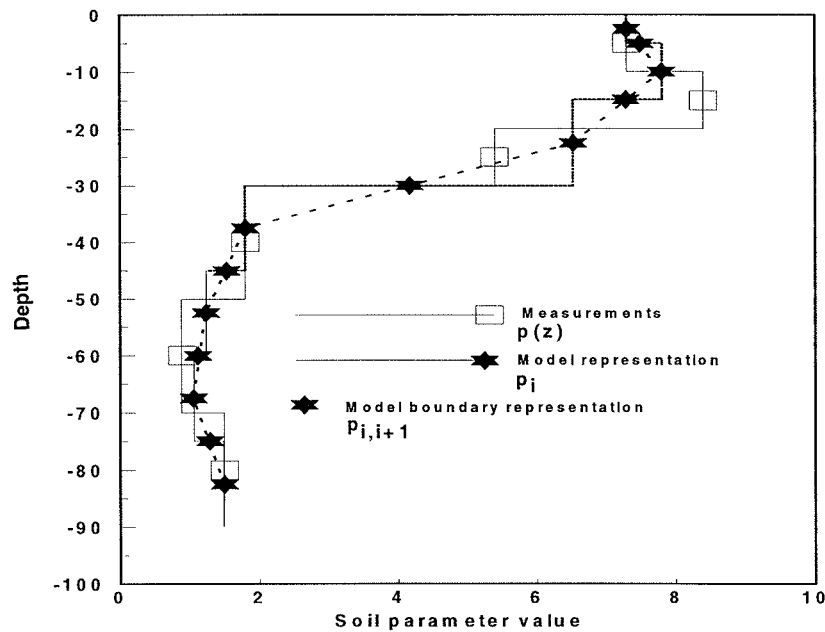
Figure 22. Graphical representation of how the model calculates soil parameters to represent a soil profile. *Grafisk återgivning av hur modellen representerar markegenskaper från uppmätta mätpunkter i en markprofil.*

4.2 Integration time step and bypass of slow processes

Integration time step must be chosen to avoid numerical instabilities in the simulation. With Euler integration one must normally choose the simulation time step equal to the shortest step necessary for the most variable condition. This may result in inconceivably long execution times, if long-term simulations are made, even for a moderate compartmentalisation of the soil. Conditional changes of the time step are made during simulation to avoid such execution times. A base time step is given initially for the simulation, but during conditions of high infiltration rates the time step is substantially decreased. Water flow rates into the top soil layer and into a layer slightly below top soil are used as tests. The occurrence of frost in the soil also decreases the time step.

In addition to conditional changes in integration time step, conditional bypasses are made to cut down execution times. If the changes in some state variable have been below a prescribed limit no flow recalculation is made. This procedure is used for water and heat flow equations separately. Since frost conditions strongly influence both water and heat flows, recalculation of both are made if any change exceeds the limit for either water or heat. Recalculation is made of flows for a number of the upper soil layers. At regular intervals the whole soil profile is updated.

5. List of symbols

5.1 Sorted by unit and description

Symbol	Description	Unit	Category	(eq)/ section	Value
α_{dry}	Albedo of dry soil		Parameter	(146)	
α_{veg}	Albedo of vegetation		Parameter	(145)	
α_r	Albedo of vegetation and soil		Parameter	(142-145)	
α_{wet}	Albedo of wet soil		Parameter	(146)	
f_{cpool}	Areal fraction of surface pool		Auxiliary, internal		
r_5	Coefficient in Ångström's formula		Parameter	(152)	
r_6	Coefficient in Ångström's formula		Parameter	(152)	
r_1	Coefficient in Brunt's formula		Parameter	(143)	
r_2	Coefficient in Brunt's formula		Parameter	(143)	
r_3	Coefficient in Brunt's formula		Parameter	(143)	
r_4	Coefficient in Brunt's formula		Parameter	(143)	
rr_1	Coefficient in Brunt's formula		Parameter	(144)	
rr_2	Coefficient in Brunt's formula		Parameter	(144)	
rr_3	Coefficient in Brunt's formula		Parameter	(144)	
rr_4	Coefficient in Brunt's formula		Parameter	(144)	
d_1	Coefficient in freezing point depression function		Parameter	(18)	
d_2	Coefficient in freezing point depression function		Parameter	(23,26)	
d_3	Coefficient in freezing point depression function		Parameter	(23,26)	
f_{umov}	Degree of compensatory uptake		Parameter	(85)	
S_e	Effective saturation		Auxiliary, internal	(41,42,43, 46)	
ψ_{eg}	Empirical coefficient used to calculate vapour pressure at soil surface		Parameter	(103)	
e_{corr}	Empirical function accounting for difference in moisture between soil surface and the middle of the uppermost layer		Auxiliary, internal	(102,103)	
q	Flow				
f_a	Fraction of air in soil		Auxiliary, internal		
f_{ci}	Impedance parameter for the effect of ice on hydraulic conductivity		Parameter	(31)	
n_{isl}	Number of soil layers considered in irrigation control		Parameter		
p_2	Parameter in water tension response function for transpiration.		Parameter	(82)	
λ	Pore size distribution index		Parameter	(23,26,41, 46,47)	
$x(i)$	Property that can be given as temporal function of $t_{day}(i)$		Parameter	(86-89)	
S_1	Radiation melt factor for old snow		Parameter	(120)	

Symbol	Description	Unit	Category	(eq)/ section	Value
e_{rat}	Ratio between potential evaporation rate and potential transpiration rate		Parameter	(113)	
f_{ret}	Retention capacity of snow		Parameter	(124)	
S_2	Snow age coefficient in radiation melt response on snow		Parameter	(120)	
i_{sfrac}	Soil irrigation fraction		Parameter		
R_T	Soil temperature response on transpiration		Auxiliary, internal	(83,84)	
t_1	Temperature coefficient when calculating R_T		Parameter	(83)	
t_2	Temperature coefficient when calculating R_T		Parameter	(83)	
i_{scov}	The degree of soil cover		Parameter		
n	Tortuosity coefficient		Property, input	(46,47)	
k	von Karman's constant		Natural constant	(76)	0.41
S_{res}	Water equivalent of snow from preceding day			(129)	
R_ψ	Water tension effect on transpiration		Auxiliary, internal	(82,84)	
pF	Water tension expressed as $\log(\psi)$		Auxiliary, internal	(40)	
c_{snow}	Addition correction coefficient for snow-precipitation		Parameter	(135)	
c_{rain}	Correction coefficient for rain precipitation	-	Parameter	(135)	
r	Degree of freezing point depression	-	Auxiliary, internal	(23,24)	
$p_{hysmaxc}$	Maximal hysteresis effect on hydraulic conductivity, log scale	-	Parameter	(56)	
p_{hysmax}	Maximal hysteresis effect on water retention, log scale	-	Parameter	(51)	
r(z)	Normalized depth distribution of water uptake	-	Parameter	(84)	
a_r	Ratio between layer thickness and unit horizontal area.	-	Auxiliary, internal	(40)	
R_i	Richardson number	-	Auxiliary, internal	(100)	
r_{frac}	Root fraction	-	Parameter	(90)	
a_{scale}	Scaling coefficient accounting for the geometry of aggregates	-	Parameter	(40)	
c_{form}	Shape coefficient	-	Parameter	(88)	
Q	Thermal quality	-	Auxiliary, output	(27,29-31)	
Q_{samin}	Thermal quality limit for snow age updating	-	Parameter		
d_{vapb}	Tortousity coefficient in diffusion equation	-	Parameter	(57)	
a	Weighting factor	-	Auxiliary, internal	(7,8,11,12)	
$t_{day}(1)$	Day number for specification of temporal variation within year.	#	Parameter	(87-89)	

Symbol	Description	Unit	Category	(eq)/ section	Value
t_{pmax}	Daynumber for maximum potential transpiration rate	#	Constant	(131)	195
q_{sol}	Layer for the ground water source flow	#	Parameter		
z_{nhp}	Layer from which heat is extracted	#	Parameter		
h_r	Relative humidity	%	Driving	(137)	
T_{hplim}	Air temperature used to calculate heat extraction from soil	°C	Constant	(156)	
T_{hpc}	Air temperature when heat extraction from soil begins	°C	Constant	(156)	11.0
T_{aamp}	Amplitude of air temperature in sine function.	°C	Parameter	(15)	
T_{amean}	Mean air temperature in sine function.	°C	Parameter	(15)	
T_{max}	Rain temperature threshold	°C	Parameter	(132)	
T_{min}	Snow temperature threshold	°C	Parameter	(132)	
T_{hp0}	Soil temperature where heat extraction ceases	°C	Parameter	(157)	
T_{hpcut}	Soil temperature where heat extraction will be reduced	°C	Parameter	(157)	
T	Temperature	°C			
T_b	Temperature at boundary between two horizons	°C	Auxiliary, internal	(11)	
T_a	Temperature of air at reference height	°C	Driving, input	(6,7)	
T_f	Temperature of fully frozen soil	°C	Constant	(20,26)	-5 °C
T_s	Temperature of soil surface	°C	Driving, input/output	(6,9,13)	
T_1	Temperature of the uppermost layer	°C	Auxiliary, internal	(7,10,13)	
$r_{\psi3}$	Surface resistance coefficient	0.001s	Parameter	(107)	
$r_{\psi1}$	Surface resistance coefficient	0.01s	Parameter	(107)	
α	Coefficient in water retention	1/cm water	Parameter	(43,48)	
ψ_c	Critical soil water tension where reduction of transpiration begins	cm water	Parameter	(82)	
ψ	Soil water tension	cm water	Auxiliary, output	(34,36,41, 43..)	
ψ_a	Soil water tension at air entry	cm water	Parameter	(41)	
ψ_m	Soil water tension at the lower boundary of Brooks & Corey's expression used	cm water	Auxiliary, internal	(45)	
ψ_x	Soil water tension at the upper boundary of Brooks & Corey's expression used	cm water	Parameter, input	(44)	
ψ_{wilt}	Soil water tension at wilting point	cm water	Natural, constant	(44)	15 000
$r_{\psi2}$	Surface resistance coefficient	cm water	Parameter	(107)	
t_{sage}	Age of snow	day	Auxiliary, Internal	(120)	
y_{cycle}	Cycle of analytical air temperature	day	Parameter	(16)	
Δ_{tp}	Duration of half period for potential transpiration	day	Constant		90
t_{ph}	Phase shift of analytical air temperature	day	Parameter	(15)	
p_1	Parameter in water tension response function for transpiration.	$day\ mm^{-1}$	Parameter	(82)	

Symbol	Description	Unit	Category	(eq)/ section	Value
a_{surf}	First order coefficient in surface runoff equation	day^{-1}	Parameter	(61)	
a_{hysk}	Age coefficient in hysteresis function	day^{-1}	Parameter	(53)	
c_v	Concentration of water vapour	$g\,m^{-3}$	Auxiliary, internal		
L_f	Latent heat of freezing	$J\,kg^{-1}$	Natural constant	(2,20,22, 23,26)	
L_v	Latent heat of vaporization	$J\,kg^{-1}$	Natural constant	(75,92,105)	
c_p	Specific heat of air (at 15 °C)	$J\,kg^{-1}\,{}^{\circ}C^{-1}$	Natural constant	(75)	1004
H	Sensible heat storage	$J\,m^{-2}$	Auxiliary, internal	(24,25,30)	
s_{h1}	Base rate of heat extraction from soil	$J\,m^{-2}\,day^{-1}$	Parameter	(155)	
R_{is}	Global radiation	$J\,m^{-2}\,day^{-1}$	Driving	(81,118, 152)	
s_h	Heat source flow in soil	$J\,m^{-2}\,day^{-1}$	Flow, output	(2)	
LE_s	Latent heat flow from soil surface	$J\,m^{-2}\,day^{-1}$	Auxiliary	(94,105)	
s_{hpmax}	Maximal heat extraction rate from soil	$J\,m^{-2}\,day^{-1}$	Parameter	(156)	
R_{nl}	Net longwave radiation	$J\,m^{-2}\,day^{-1}$	Auxiliary, internal	(143,144)	
R_n	Net radiation	$J\,m^{-2}\,day^{-1}$	Auxiliary, internal	(75,141)	
R_{Na}	Net radiation at reference height	$J\,m^{-2}\,day^{-1}$	Driving	(91)	
R_{ns}	Net radiation at soil surface	$J\,m^{-2}\,day^{-1}$	Auxiliary	(91,92,105)	
R_{nsh}	Net shortwave radiation	$J\,m^{-2}\,day^{-1}$	Auxiliary, internal	(142)	
R_{pris}	Potential global radiation (no atmosphere)	$J\,m^{-2}\,day^{-1}$	Function	(153)	
H_s	Sensible heat flow	$J\,m^{-2}\,day^{-1}$	Auxiliary	(93)	
q_h	Soil heat flow, between layers	$J\,m^{-2}\,day^{-1}$	Flow, output	(1,10, 13,14)	
$q_h(low)$	Soil heat flow, lower boundary	$J\,m^{-2}\,day^{-1}$	Parameter	2.1.5	
s_{h2}	Air temperature dependence of heat extraction from soil	$J\,m^{-2}\,day^{-1}\,{}^{\circ}C^{-1}$	Parameter	(145)	
f_{lat}	Fraction of latent heat to total heat storage at T_f	$J\,m^{-2}/(J\,m^{-2})$	Auxiliary, internal	(22)	
E_f	Energy storage of frozen soil at temperature T_f	$J\,m^{-3}$	Auxiliary, internal	(20,22,23)	
E	Energy storage of soil. Expressed relative to a level at 0°C and fully unfrozen soil	$J\,m^{-3}$	State, output	(23,24,30)	
E_1	Energy storage of uppermost soil layer	$J\,m^{-3}$	State	(26)	
C	Heat capacity	$J\,m^{-3}\,{}^{\circ}C^{-1}$	Auxiliary, internal	(1-3)	
C_f	Heat capacity of frozen soil	$J\,m^{-3}\,{}^{\circ}C^{-1}$	Auxiliary, internal	(19,20,25)	
C_i	Heat capacity of ice	$J\,m^{-3}\,{}^{\circ}C^{-1}$	Natural constant	(19,26)	
C_s	Heat capacity of solid material	$J\,m^{-3}\,{}^{\circ}C^{-1}$	Auxiliary, internal	(1, 3,19)	

Symbol	Description	Unit	Category	(eq)/ section	Value
C_w	Heat capacity of water	$J\,m^{-3}\,°C^{-1}$	Natural constant	(3,19)	$4.2\,10^6$
g_{ris}	Half saturation for global radiation	$J m^{-2} day^{-1}$	Parameter	(81)	
w_i	Mass of ice	$kg\,m^{-2}$	State, internal	(20,21,23, 30)	
w	Mass of water	$kg\,m^{-2}$	State, output	(21)	
S_{wlmin}	Threshold liquid water storage of snow, controlling soil surface temperature	$kg\,m^{-2}$	Parameter		
ρ_a	Density of air (at 15 °C)	$kg\,m^{-3}$	Natural constant	(75,93,94)	1.220
ρ_{water}	Density of liquid water	$kg\,m^{-3}$	Natural constant	(21)	1000
ρ_{prec}	Density of precipitation (mixture snow + rain)	$kg\,m^{-3}$	Auxiliary, internal	(127)	
ρ_{old}	Density of snow from preceding day	$kg\,m^{-3}$	Auxiliary, internal	(129,130)	
ρ_s	Dry bulk density	$kg\,m^{-3}$	Auxiliary, internal	(5,28)	
s_{dl}	Liquid water coefficient in snow density function	$kg\,m^{-3}$	Parameter	(129)	
ρ_{snow}	Snow density	$kg\,m^{-3}$	Auxiliary, internal	(125,126)	
ρ_{smin}	Snow density of newly formed snow	$kg\,m^{-3}$	Parameter	(127)	
k_{rn}	Extinction coefficient for net radiation	LAI^{-1}	Parameter	(91)	
d_p	Characteristic distance when calculating q_{wp}	m	Parameter	(64)	
d_a	Damping depths of soil	m	Auxiliary, internal	(15,17)	
z	Depth	m	Internal	(1,2,..)	
z_{sat}	Depth of ground water table	m		(63,64)	
z_2	Depth where the base flow of q_{gr} ceases	m	Parameter	(74)	
z_1	Depth where the peak flow of q_{gr} ceases	m	Parameter	(74)	
d	Displacement height	m	Auxiliary, Parameter	(76)	
z_p	Level of drainage pipes	m	Parameter	(64-67)	
z_{ref}	Reference height for climatic data	m	Parameter	(76)	
m_f	Refreezing efficiency coefficient in snow melt function	m	Parameter	(119)	
z_r	Root depth	m	Parameter (driving)	(90)	
z_0	Roughness length	m	Parameter	(76)	
Δ	Thickness	m			
Δ_h	Thickness of humus layer	m	Parameter	(12,13,98)	
Δz_{prec}	Thickness of precipitation (snow + rain)	m		(126,128)	
Δz_{snow}	Thickness of snow	m	State, output	(8,9,119)	
Δz_{cov}	Thickness of snow when covering the total area	m	Parameter	(9)	
z_1	Thickness of uppermost soil layer	m	Parameter	(10,14)	
Δz_{old}	Thickness snow pack from preceding day	m		(126,130)	

Symbol	Description	Unit	Category	(eq)/ section	Value
s_{dw}	Water equivalent coefficient in snow density function	m^{-1}	Parameter	(129)	
D_0	Diffusion coefficient for vapour in free air	$m^2 s^{-1}$	Natural constant		
D	Thermal diffusivity of soil	$m^2 s^{-1}$	Auxiliary, internal	(17)	
f_s	Fraction of soil material	m^3/m^3	Auxiliary, internal	(3)	
i_{am}	Amount of automatic irrigation	mm	Parameter		
$f_{wcovtot}$	Amount of water corresponding to complete areal cover	mm	Parameter	(62)	
W_{pool}	Amount of water in surface pool	mm	State, output	(61,62)	
s_{smin}	Critical soil water storage used for irrigation control	mm	Parameter		
S_i	Interception storage	mm	Auxiliary	(110,114)	
S_{imax}	Interception storage capacity	mm	Auxiliary	(110)	
S_{wlres}	Residual amount of liquid water in snow at the end of a day	mm	Auxiliary	(121,123)	
W_{pmax}	Residual water storage on soil surface	mm	Parameter	(61)	
S_{def}	Surface moisture deficit	mm	Parameter	(104)	
S_{excess}	Surface moisture excess	mm	Parameter	(104)	
S_{wlmax}	The total water retention capacity of snow	mm	Auxiliary, internal	(122,124)	
S	Water equivalent of snow	mm	State	2.9	
Ei_a	Actual evaporation rate from intercepted water	$mm\ day^{-1}$	Auxiliary	(114)	
TR_a^*	Actual transpiration rate (excluding compensatory uptake)	$mm\ day^{-1}$	Auxiliary	(84,85)	
TR_a	Actual transpiration rate (including compensatory uptake)	$mm\ day^{-1}$	Auxiliary	(85)	
S_{wl}	Daily accumulation of liquid water in snow	$mm\ day^{-1}$	Auxiliary, internal	(121)	
E_s	Evaporation from soil surface	$mm\ day^{-1}$	Flow	(94,105, 108, 117)	
ET	Evapotranspiration, $EI_a + E_s + TR_a$	$mm\ day^{-1}$	Auxiliary	(117)	
q_{sof}	Ground water source flow	$mm\ day^{-1}$	Parameter	2.3.8	
q_{gr}	Groundwater sink flow	$mm\ day^{-1}$	Auxiliary	(74)	
i_{ar}	Intensity of automatic irrigation	$mm\ day^{-1}$	Parameter		
S_{int}	Interception rate	$mm\ day^{-1}$	Auxiliary	(110,112, 114)	
P_{samin}	Limit for snow age updating	$mm\ day^{-1}$	Parameter		
q_2	Maximum flow rate for base flow in q_{gr}	$mm\ day^{-1}$	Parameter	(74)	
q_1	Maximum flow rate for peak flow in q_{gr}	$mm\ day^{-1}$	Parameter	(74)	
Tr_{pmax}	Maximum potential transpiration rate	$mm\ day^{-1}$	Constant	(131)	4
P_m	Measured precipitation	$mm\ day^{-1}$	Driving	(135)	
M	Melting rate of snow	$mm\ day^{-1}$	Auxiliary, internal	(118)	
Ei_p	Potential evaporation rate from intercepted water	$mm\ day^{-1}$	Auxiliary	(113,114)	

Symbol	Description	Unit	Category	(eq)/ section	Value
$TR_p{}^*$	Potential transpiration after adjusting for evaporation of intercepted water	mm day^{-1}	Auxiliary	(84,85, 113,116)	
TR_p	Potential transpiration rate	mm day^{-1}	Driving, internal	(75,113)	
P	Precipitation	mm day^{-1}	Auxiliary	(133-135)	
P_r	Rain precipitation	mm day^{-1}	Auxiliary, internal	(133)	
k_{sat}	Saturated conductivity of soil	mm day^{-1}	Property, input	(49)	
k_{mat}	Saturated conductivity of soil matrix, excluding effects of macropores	mm day^{-1}	Property, input	(40,46, 47,48)	
q_{bypass}	Soil water flow in macropores	mm day^{-1}	Auxiliary, internal	(37,39)	
q_{mat}	Soil water flow in matrix	mm day^{-1}	Auxiliary, internal	(36,38,39)	
q_{in}	Soil water flow to a soil layer in macropores or as infiltration rate.	mm day^{-1}	Auxiliary, internal	(36)	
$q_{wp}(I)$	Soil water flow to drainage pipe	mm day^{-1}	Flow, output	(63)	
q_w	Soil water flow, between layers	mm day^{-1}	Flow, output	(34,35)	
S_{mat}	Sorptivity capacity of aggregates	mm day^{-1}	Auxiliary, internal	(38,40)	
q_{surf}	Surface runoff from surface pool	mm day^{-1}	Flow, output	(61)	
q_{wp}	Total water flow to drainage pipe	mm day$_{-1}$	Auxiliary	(64)	
k_{wf}	Unsaturated conductivity of partially frozen soil	mm day^{-1}	Auxiliary, internal	(31)	
k_w	Unsaturated conductivity of soil	mm day^{-1}	Auxiliary, internal	(31,32,34, 36,46-50)	
m_T	Temperature coefficient in snow melt function	mm day^{-1} °C^{-1}	Parameter	(119)	
M_T	Temperature influence function on snow melting	mm day^{-1} °C^{-1}	Auxiliary, internal	(118,119)	
m_{Rmin}	Minimum value of Global radiation influence in snow melt function	mm J^{-1}	Parameter	(120)	
M_R	Radiation influence function on snow melting	mm J^{-1} m^2	Auxiliary, internal	(118,120)	
i_{LAI}	Specific interception storage capacity of canopy	mm LAI^{-1}	Parameter	(111)	
δ_{surf}	Surface water balance	mm water	Auxiliary	(104)	
s_w	Net water source flow in soil	mm^{-2} day^{-1}	Flow, output	(35)	
u	Wind speed	ms^{-1}	Driving, input	(76)	
g_{max}	Maximal stomatal conductance	ms^{-1}	Parameter	(81)	
g_l	Stomatal conductance	ms^{-1}	Auxiliary, internal	(80, 81)	
g	Gravitational constant	ms^{-2}	Natural constant		9.81
$e_s(T)$	Saturation vapour pressure function	Pa	Natural constant	(139,140)	
e_a	Vapour pressure air at reference height	Pa	Auxiliary (Driving)	(75,94, 105, 137)	
e_{surf}	Vapour pressure at soil surface	Pa	Auxiliary	(94,102)	
δe_a	Vapour pressure deficit	Pa	Auxiliary	(138)	

Symbol	Description	Unit	Category	(eq)/ section	Value
g_{vpd}	Vapour pressure deficit response on stomatal conductance	Pa	Parameter	(81)	
e_v	Vapour pressure in soil	Pa	Auxiliary		
γ	Psycrometric constant	$Pa\ °C^{-1}$	Natural constant	(75,94)	66.
Δ	Slope of saturated vapour pressure versus temperature curve	$Pa\ °C^{-1}$	Natural property	(75)	
r_{as}	Aerodynamic resistance between reference height and soil surface	$s\ m^{-1}$	Auxiliary	(93,105)	
r_a	Aerodynamic resistance between reference height and vegetation	$s\ m^{-1}$	Auxiliary	(75,76)	
r_{ab}	Aerodynamic resistance between vegetation and soil surface	$s\ m^{-1}$	Auxiliary	(99,101)	
r_{alai}	Increase of aerodynamic resistance below canopy per LAI of canopy	$s\ m^{-1}$	Parameter	(101)	
r_s	Surface resistance	$s\ m^{-1}$	Auxiliary	(75)	
r_ψ	Surface resistance coefficient	$s\ m^{-1}$	Parameter	(106)	
r_{sint}	Surface resistance for intercepted water	$s\ m^{-1}$	Parameter	2.8	
r_{ss}	Surface resistance, soil surface	$s\ m^{-1}$	Auxiliary	(105-107)	
ω	Angle frequency	s^{-1}	Auxiliary, internal	(15-17)	
θ_{ice}	Ice content	vol %	Auxiliary, internal	(2,19)	
θ_l	Liquid water content	vol %	Auxiliary	(3,4,5..)	
θ_{tf}	Liquid water content at the temperature T_f	vol %	Auxiliary, internal	(18,19,21)	
a_{PF1}	Lower threshold in hysteresis function	vol %	Parameter	(54)	
θ_m	Macro pore volume	vol %	Parameter	(45,49)	
a_{thetm}	Rate at which maximal hysteresis has developed	vol %	Parameter	(55)	
θ_r	Residual soil water content	vol %	Parameter	(42)	
a_{PF2}	Upper limit in hysteresis function	vol %	Parameter	(54)	
θ_s	Water content at saturation	vol %	Parameter	(42,44)	
θ_x	Water content at the upper boundary of the Brooks & Corey's expression	vol %	Auxiliary, internal	(44)	
θ_w	Water content at wilting point (15 atm)	vol %	Parameter	(18,44)	
k_h	Thermal conductivity	$W\ m^{-1}\ °C^{-1}$	Property, internal	(1,8,29)	
b_1	Thermal conductivity coefficient for mineral soil, frozen	$W\ m^{-1}\ °C^{-1}$	Property, input	(28)	
b_2	Thermal conductivity coefficient for mineral soil, frozen	$W\ m^{-1}\ °C^{-1}$	Property, input	(28)	
b_3	Thermal conductivity coefficient for mineral soil, frozen	$W\ m^{-1}\ °C^{-1}$	Property, input	(28)	
b_4	Thermal conductivity coefficient for mineral soil, frozen	$W\ m^{-1}\ °C^{-1}$	Property, input	(28)	
a_1	Thermal conductivity coefficient for mineral soil, unfrozen	$W\ m^{-1}\ °C^{-1}$	Property, input	(5)	
a_2	Thermal conductivity coefficient for mineral soil, unfrozen	$W\ m^{-1}\ °C^{-1}$	Property, input	(5)	
a_3	Thermal conductivity coefficient for mineral soil, unfrozen	$W\ m^{-1}\ °C^{-1}$	Property, input	(5)	
h_1	Thermal conductivity coefficient for organic soil, unfrozen	$W\ m^{-1}\ °C^{-1}$	Property, input	(4)	

Symbol	Description	Unit	Category	(eq)/section	Value
k_{hi}	Thermal conductivity of frozen soil	$W\,m^{-1}\,{}^{\circ}C^{-1}$	Property, internal	(28,29)	
k_{hm}	Thermal conductivity of mineral soil, unfrozen	$W\,m^{-1}\,{}^{\circ}C^{-1}$	Property, internal	(5,10, 12,29)	
k_{Ho}	Thermal conductivity of organic soil	$W\,m^{-1}\,{}^{\circ}C^{-1}$	Property, internal	(4,12,13, 14,27)	
k_{snow}	Thermal conductivity of snow	$W\,m^{-1}\,{}^{\circ}C^{-1}$	Property, internal	(8)	
k_{hw}	Thermal conductivity of unfrozen soil	$W\,m^{-1}\,{}^{\circ}C^{-1}$	Property, internal	(29)	
h_2	Thermal conductivity coefficient for organic soil, unfrozen	$W\,m^{-1}\,{}^{\circ}C^{-1}\,vol\,\%^{-1}$	Property, input	(4)	
α_h	Heat transfer coefficient	$W\,m^{-1}\,{}^{\circ}C^{-1}$	Parameter	(33)	
σ	Stefan-Boltzmann's constant	$Wm^{-2}K^{-1}$	Natural constant	(143,144)	5.67×10^{-8}
s_k	Thermal conductivity coefficient for snow.	$Wm^4 kg^{-2}$	Parameter	(125)	

6. Acknowledgement

The development of the SOIL model is the result of many years of work with many different people involved. Only the most important will be mentioned below but I fully appreciate all contributors to the model development. In the initial phase of the work Sven Halldin made substantial contributions which is reflected in the early reports (e.g. Jansson & Halldin, 1979). During later years many users of the model have contributed with ideas and suggestions that have resulted in model improvements. For instance: Lars-Christer Lundin and Manfred Stähli concerning frost in the soil; Bo Thunholm and Gunnel Alvenäs concerning soil surface temperature; Peter Boterweg, Bengt Espeby, Annemieke Gärdenäs, Holger Johnsson, Nicholas Jarvis, Gunn Persson, Christina Thoms-Hjärpe, Lisbet Lewan, Anders Lindroth and Malcolm McGechan concerning various parts of the model.

Comments and constructive criticism of this report was given by Nicholas Jarvis, Henrik Eckersten and Annemieke Gärdenäs.

Special thanks are given to Kerstin Berglund, the editor of the series of Reports from the Division of Agricultural Hydrotechnics, who showed a lot of patience during the final crucial stage of word-processing.

7. Summary in Swedish (Sammanfattning)

En matematisk modell som används för att beräkna flöden och lagring av vatten i systemet mark-växt-atmosfär utgår från fysikaliska principer och mer eller mindre kända kunskaper om fysikaliska processer. Modellen finns programmerad för körning med IBM-PC kompatibel dator. Denna rapport ger en utförlig beskrivning av modellen medan en annan rapport (Jansson, 1991) ger en beskrivning om hur modellens används.

7.1 Modellens Struktur

Soil modellens struktur utgår ifrån marken uppdelad i ett antal skikt som behandlas separat för vatten och värme. För att beskriva gränsytorna till marken behandlas också vegetation, snötäcke och eventuell vattenanhopning på markytan. Marken inkluderar både den omättade och mättade delen av markprofilen.

7.2 Markfysikaliska egenskaper

Modellen utgår från de partiella differentialekvationer som beskriver vatten- och värmeflöden i en markprofil. Ekvationen löses med en numerisk teknik där derivator med avseende på djupet och på tiden approximeras med små differenser.

Två markfysikaliska samband måste vara kända för att ekvationen skall kunna lösas, nämligen pF-kurvan (: ψ = f (θ)]) och den mättade och omättade konduktiviteten (: K sub w = f (ψ)] eller : k sub w = f (θ)]).

7.3 Vegetationen och markytan

Vegetationen kan fysikaliskt ses som en länk mellan det vatten som finns i marken och den vattenånga som finns i luften. Vegetationens roll vid flödet av vatten från mark till atmosfär kan i huvudsak beskrivas genom väl accepterade fysikaliska teorier. Man utgår ifrån vad som kallas mark - växt - atmosfär - kontinuiteten. Denna innebär att flödet sker från ett högt potentialtillstånd i marken mot ett lägre tillstånd i växten och ytterligare lägre i atmosfären. Övergångarna mellan dessa tillstånd styrs av motstånd eller resistanser. Denna tankemodell brukar kallas SPAC som står för Soil - Plant -Atmosphere Continuum.
I en matematisk modell typ SOIL-modellen tas inte hänsyn till vattenflödet hela vägen från mark till atmosfär, utan man har valt en förenkling som innebär att endast de viktigaste delarna av flödesbanan är beaktade. Det potentiella eller möjliga flödet beräknas med en matematisk formel för avdunstning. Den utgår ifrån det arbete som Penman utförde under 40- och 50-talen i England.
Begränsningar i flödet som uppkommer genom motstånd i marken, i roten, i växten eller vid vattnets övergång från växt till atmosfär är sammanfattade i olika empiriska reduktionsfaktorer.
För att efterlikna olika typer av vegetationstäcken kan man ange de olika egenskaperna som finns medtagna i modellen, genom olika parametervärden. De viktigaste parametrarna för att förklara skillnader mellan olika vegetationstäcken är de som ger bladytans storlek och ytresistansens värde. Även rotfördelningen är viktig, men den inverkar främst genom att det totala förrådet av växttillgängligt vatten påverkas.
I figur 20 visas hur olika flöden och resistanser är representerade i modellen.

7.3.1 Potentiell avdunstning

Potentiell avdunstning beräknas med en kombinationsformel som tar hänsyn till den energi som finns tillgänglig för vattnets fasomvandling och till den grad av effektivitet med vilken borttransport av vattenånga kan ske.
Ekvationen som används för att få ett värde på potentiell avdunstning kallas ofta för Penman-Monteiths formel (se ekvation 48)
Kombinationsformeln för potentiell avdunstning används på olika sätt för att beräkna tre bidrag till den totala avdunstningen.
1)   Evaporation av på växten intercepterat vatten.
2)   Evaporation av vatten från markytan.
3)   Transpiration genom växten.

Det som beskriver skillnaden i potentiell avdunstning från de olika källorna av vatten är dels den tillgängliga strålningsenergin, : R_n, och de båda resistanserna som anger transportmotstånden i gränsytan mellan vegetation och luft (: r_s) och luft ovan beståndet (: r_a).
Först fördelas strålningsenergin, : R sub n], mellan bestånd och markyta enligt en exponentiell funktion (se ekvation 60). Den del av energin som absorberas av beståndet är tillgänglig för evaporation av intercepterat vatten eller transpiration av vatten via växten. Evaporation av intercepterat vatten sker utan eller med ett mycket litet transportmotstånd vid gränsytan mot luften. Därvid förbrukas en given mängd av tillgänglig energi om vatten förekommer på växtytan. Mängden av tillgänglig energi (givet av stålningsbalansen) som förbrukas motsvarar dock bara en del av den energi som åtgått vid fasomvandlingen. Detta beror av möjligheten att ta energi direkt ur luften vid hög turbulens och vid god tillgång på vatten (Luften kyls genom avdunstningen; jfr uppstigandet ur badet på blåsig strand).
Den aerodynamiska resistansen, : r sub a], för transpiration och evaporation från bladytor beräknas från vindhastigheten och ytans skrovlighet (se ekvation 49).

73

7.3.2 Markyteavdunstning

Avdunstningen från markytan är en komplex process där markens egenskaper i hög grad kommer att bestämma förutsättningarna. För att utföra den beräkningen finns två olika valmöjligheter i modellen, en mer empirisk som grundar sig på samma kombinationsformel som används för potentiell avdunstning och en som i högre grad grundar sig direkt på de fysikaliska ekvationerna för transport av värme och vatten i atmosfär och mark. Båda grundar sig på en lösning av energibalansekvationen för markytan men den empiriska utgår från en analytisk lösning med hjälp av kombinationsformeln medan den mer mekanistiska utgår från en numerisk lösning av i grunden samma ekvationer. I bägge dessa fall måste hänsyn tas till energilagring i marken och upptorkningen närmast markytan. Detta görs på lite olika sätt i de bägge ansatserna som beskrivs nedan.

Gemensamt för båda ansatserna är att om ett vegetationstäcke finns så måste den aerodynamiska resitansen mellan markytan och referensnivån ta hänsyn till detta. Resistansen, : r_{as}, är beroende av den totala bladytan, LAI, och luftens skiktning (se ekvationerna 67 och 68).

7.3.2.1 Ansats byggd på kombinationsformel

Avdunstningen från markytan beräknas med kombinationsformeln (ekvation 73) utgående från den tillgängliga strålningsenergin, : R_{ns} och värmeflödet från marken, : q_h. Värmeflödet från marken är delvis ett resultat av avdunstningen från markytan och för att kunna hantera detta så utnyttjas modellen beräknade värmeflöde från föregående tidssteg (t-1) vid beräkningen av avdunstningen vid tidpunkten (t). Genom att modellen normalt har ett betydligt mindre tidssteg än vad som motsvaras av upplösningen i de meteorologiska variablerna som oftast är medelvärden av en timme eller ett dygn föranleder detta normalt ingen större onoggrannhet i den beräknade avdunstningen.

För beräkning av markyteavdunstningen, : LE_s, med kombinationsformeln definieras en resistans för vattenångflöde vid markytan. Markytans ytresistans, : r_{ss}, beror i hög grad på tillgången av vatten på markytan och i det översta markskiktet. I modellen beräknas : r_{ss} som en funktion av vattenpotential i markens översta skikt och en massbalansberäkning för markytan som indikerar markytans fuktighet (se ekvationerna 72 och 74).

Värmeflödet, : q_h kan därefter beräknas på två sätt. Det enklaste möjligheten förutsätter ingen koppling till avdunstningen utan utgår från att markytans temperatur är densamma som luftens temperatur. Denna ansats kan ge stora fel både för beräkningen av markens temperatur och för beräkningen av markyteavdunstningen. Den fysikaliskt rimligare lösningen är att utgående från den beräknade avdunstningen utnyttja den därvid implicit antagna yttemperaturen för beräkning av värmeflödet till marken. Detta göres genom att det sensibla flödet, : H_s erhålles från energibalansen (se ekvation 76).

7.3.2.2 Ansats byggd på numerisk lösning

Den numeriska ansatsen bygger på att energibalansekvationen för markytan löses genom ett iterativt förfarande.

För att lösa denna ekvation så varieras markytans temperatur, : T_s enligt ett givet schema. Först ansättes : T_s som lika med : T_a och därefter beräknas alla ingående termer enligt deras respektive ekvationer. Den erhållna summan av : H_s : LE_s och : q_h jämförs med : R_{ns} och beroende på avvikelsen så skattas ett nytt värde för : T_s. Denna procedur upprepas ända tills dess att avvikelsen mellan : R_{ns} och summan av de tre energiflödena är mycket liten. Normalt erhålles ett fel på mindre än 0.1 °C efter cirka 15 iterationer. Vattenångtrycket vid markytan beräknas av markens yttemperatur, T_s, och markvattnets tension i det

översta skiktet och en empirisk korrektionsfaktor, e_{corr}, som tar hänsyn till stora gradienter i fuktighet nära markytan (se ekvationerna 70 - 72).

7.3.3 Avdunstning av intercepterat vatten

Ytresistansen för intercepterat vatten är mycket låg och bestäms av parametern : r_{sint}. För transpirationen från en växt med god vattentillgång är ytresistansen i allmänhet betydligt högre.

7.3.4 Aktuell transpiration

För att kunna beskriva hur vattnet tas upp från marken anges rötternas fördelning i olika skikt och dessutom hur begränsningen av vattenupptaget sker då växten inte längre förmår att ta upp vatten till den potentiella nivån som beräknats med Penman-Monteith's formel. Aktuell (verklig) vattenupptagning från

ett markskikt, : W_{upt} (i)] beräknas utgående från responsfunktioner som tar hänsyn till marktemperaturen, markvattenpotentialen, skiktets andel av det totala rotsystemet (se ekvation 53)

7.4 Avrinning och behandling av grundvatten

Avrinningen från en markprofil kan beräknas på flera olika sätt allt efter vilken information som finns om marken och vilka lokala geologiska dräneringsförhållanden som råder på platsen som skall efterliknas. En stor förenkling som är gjord är att modellen ej tar hänsyn till horisontella skillnader i vattenhalter och vattenflöden. Modellen kan i detalj beskriva hur vattnet fördelar sig vertikalt genom att den partiella differentialekvationen löses med avseende på markdjup och tid. Ett horisontellt vattenflöde beräknas endast som ett netto i modellen (dvs skillnaden mellan in- och utflöde för en given nivå). Ett flöde till ett dike eller till ett grundvattenrör betraktas därför i ekvationen som en sänkterm på samma sätt som rötterna. Den stora skillnaden är att sänktermen för dränering endast är aktuell i den mättade zonen av marken medan sänktermen för vattenupptagning via rötter är aktuell för den omättade zonen.

Flödet från ett vattenmättat skikt i med tjockleken Δz och med mättad hydraulisk konduktivitet : k_s (i)] till en dräneringsledning eller dike på nivån : z_p beräknas med en ekvation som bygger på Dacrys lag (se ekvation 46).

Darcys lag som också används för att beräkna det vertikala flödet i den omättade zonen. Avståndet l kan skattas på olika sätt allt efter vilken typ av flöde som skall beräknas. Ibland kan l väljas för att motsvara markytans lutning och därmed den gradient som styr ett naturligt dränerande grundvattenflöde. I andra fall, då vi exempelvis har dräneringsledning eller diken med fasta avstånd kan l skattas utgående från den form som grundvattenytan antar mellan två dräneringsledningar.

För att få det totala flödet till dräneringsledningarna summeras bidragen från alla mättade nivåer. Vertikala flöden mellan mättade skikt beräknas så att endast det skikt som gränsar till den omättade zonen kommer att få en förändrad vattenhalt.

Det är under naturliga förhållanden vanligt att grundvattenströmningen kan ske mot olika typer av sänkor i terrängen som är betingade av lokala geologiska förhållanden och inte bara mot ytliga diken och dräneringsledningar som kan finnas. För att hantera detta flöde kan flödet till dräneringsledningarna, : q_{wp}, kombineras med ytterligare ett flöde i modellen, : q_{gr}, vilket beräknas med en ekvation av typen 1:a ordningen. Denna ekvationstyp används mycket inom hydrologin för att beskriva flödets variation i bäckar och vattendrag. I ord innebär 1:a ordningens ekvation i här aktuellt fall att flödet vid en given tidpunkt är proportionellt mot ett tillstånd som beskriver mängden vatten som kan dräneras (se ekvation 47).

Denna empiriskt funna ekvation kan användas för att efterlikna olika typer av akvifärerer utan att vi behöver använda de strikt fysikaliska egenskaperna som definieras genom Darcys lag för vattenflöden i mark. Ekvationen är speciellt lämplig att använda för djupare skikt i marken där vi ofta saknar god information om de faktiska fysikaliska egenskaperna. I modellen används denna formel för flödet under dräneringsledningarnas nivå, vilket har fördelen att vi också kan behandla flöden som dränerar marken på djupare nivåer.

8. References

Axelsson, B. & Ågren, G., 1976. Tree growth model (PT 1) - a development paper. - Swed. Conif. For. Proj. Int. Rep. 41, 79 pp.

Beskow, G., 1935. Soil freezing and frost heaving with special application to roads and railroads. Sveriges Geologiska Undersökning, serie C, No 375, Årsbok 26(3), 242 pp. (In Swedish)

Brooks, R. H. & Corey, A. T. 1964. Hydraulic properties of porous media, Hydrology Paper No. 3, Colorado State University, Fort Collins, Colorado, 27 pp.

de Vries, D. A., 1975. Heat transfer in soils. - In: de Vries,D. A. and Afgan, N. H. (Eds.) Heat and Mass Transfer in the Biophere. I. Transfer Processes in Plant Environment, pp. 5-28. Washington D. C.:Scripta Book Co.

Ernst, L.F. 1956 Calculation of the steady flow of groundwater in vertical cross sections. Netherlands Journal of Agricultural Science. 4: 126-131.

Harlan, R. L., 1973. Analysis of coupled heat-fluid transport in partially frozen soil. Water Resour. Res. 9:1314-1323.

Haverkamp, R. & Vauclin, M. 1979. A note on estimating finite difference interblock hydraulic conductivity values for transient unsaturated flow problems. - Water Resour. Res. 15 (1):181-187.

Hooghoudt, S. B. 1940. Bijdragen tot de kennis van enige natuurkundige grootheden van de ground No. 7 Versl. Landb. Onderz. 42: 449-541.

Impens, I. and Lemeur, R. 1969. Extinction of net radiation in different crop canopies. Arch. Geoph. Bioklimatol., Ser. B., 17: 403-412.

Kersten, M. S. 1949. Thermal properties of soils. Inst. of Technology, Eng. Exp. Station, Bull. No. 28, 26 pp., Minneapolis: Univ. Minnesota.

Monteith, J.L. 1965. Evaporation and environment. In: Fogg, G.E. (Editor) The State and Movement of Water in Living Organisms, 19th Symp. Soc. Exp. Biol., pp. 205-234. Cambridge: The Company of Biologists.

Mualem, Y. 1976. A new model for predicting the hydraulic conductivity of unsaturated porous media. - Water Resour. Res. 12:513 - 522.

Richards, L.A. 1931. Capillary conduction of liquids in porous mediums. - Physics. 1:318-333.

Snow Hydrology 1956. Summary reports of the snow investigations. Portland, Oregon: North Pacific Division, Corps of Engineers, U.S. Army, 437 pp.

Youngs, E.G. 1980. The analysis of groundwater seepage in heterogeneous aquifers. Hydrological Sciences, Bullentin 25:155-165.

Wankiewicz, A., 1979. A review of water in snow. In: S. C. Colbeck and M. Ray (eds.) Proc: Modeling snow cover runoff, U. S. Army, Corps of Engineers, CRREL, Hanover, New Hamphire. pp. 222-252.

9. Bibliography

This list includes documents where the SOIL model has been used or where the model is described independent if they are quoted in the text or not.

Alavi, G. 1995. Radial stem growth and transpiration of Norway spruce in relation to soil water availability. Communications 95:8, 42 p.

Alavi, G. 1996. Radial stemgrowth of Norway spruce in relation to spatial variation in soil moisture conditions. Scand. J. of Forest Research. 11: 209-219.

Alavi, G. & Jansson, P.-E. 1995. Transpiration and soil moisture dynamics. for spruce stands of different canopy densities and water availability. In: Nilsson, L-O., Hüttl, R. F., Johansson, U.T. and Mathy, P. (eds). Nutrient Uptake and Cycling in Forest Ecosystem. Ecosystem research report 21:41-51. Luxemburg, ISBN 92-826-9416-X

Alvenäs, G. 1994. The interaction between soil moisture and surface conditions. In Persson. R. (ed.) Proceedings of NJF-seminar no 247: Agrohydrology and nutrient balances, October 18-20, 1994, Uppsala, Sweden. p.93. Swedish University of Agricultural Sciences, Division of Agricultural Hydrotechnics, Communications 94:5.

Alvenäs, G., Johnsson, H. & Jansson, P.E. (1986). Meteorological conditions and soil climate of four cropping systems: Measurements and simulations from the project "Ecology of Arable Andersson, J. 1991. Avdunstning från energiskog. Nödvändig detaljeringsgrad i modellansättningen. Division of Hydrology, Report Series A 52, Uppsala University, Department of Hydrology, 54 pp.

Alvenäs, G & Marstorp, H. 1993. Effect of a ryegrass catch crop on soil inorganic-N content and nitrate leaching. Swedish J.agric Res., 23:3-14.

Alvenäs, G. & Jansson, P.-E. 1997. Model for evaporation, moisture and temperature of bare soil: calibration and sensitivity analysis. Agric. For. Met., 88: 47-56.

Blombäck, K., Stähli, M. and Eckersten, H. 1995. Simulation of water and nitrogen flows and plant growth for a winter wheat stand in central Germany, Ecological Modelling, 81:157-167.

Blombäck, K & Eckersten, H. 1997. Simulated growth and nitrogen dynamics of perennial rye grass. Agricultural and Forest Meteorology, 88:37-45.

Borg, G. Ch. & Jansson, P-E. 1991. Simulation of moisture and temperature conditions in a clay arable soil, STRIAE, University of Uppsala (in press)

Borg, G. Ch., Andersson, B.I., Hultberg, H. 1995. Modelling the effects of changing climate on the hydrological and thermal properties in soil. In: Global change and Arctic terrestrial ecosystems, Proceedings of Papers Contributed to the International Conference, 21-26 August 1993, Oppdal, Norway, European Commission, DG- X11, Brussels, EUR 15519 EN: 255-261.

Bouten, W. & Jansson, P-E. 1995. Water balance of the Solling spruce stand as simulated with various forest-soil-atmosphere models. Ecological Modelling, 83: 245-253.

Bergström, L. & Jarvis, N. 1991. Prediction of nitrate leaching losses from arable land under different fertilization intensities using the SOIL/SOILN models. Soil Use and Management 7:79-85.

Blombäck, K. 1994. Simulation of grass growth and its influence on soil mineral nitrogen. NJF-seminar 245. The use of catch or cover crops to reduce leaching and erosion. Ar/Knivsta, Sverige, 3-4 oktober 1994. NJF-utredningar/rapporter no. 99.

Blombäck, K. 1994. Grass growth and its influence on soil mineral nitrogen. A simulation study. In Persson, R. (ed.) Proceedings of NJF-seminar no 247: Agrohydrology and nutrient balances, October 18-20, 1994, Uppsala, Sweden, p.115. Swedish University of Agricultural Sciences, Division of Agricultural Hydrotechnics, Communications 94:5.

Botterweg, P.F. 1988. The SOIL-CREAMS model to simulate soil and chemical losses from agricultural areas. Proceedings of the International Symposium on water quality modeling of argricultural non-point sources. 1988, Utah State University, Logan, Utah, Donn. G. Decoursey (ed). ARS-81

Botterweg, P.F. 1989. The SOIL/CREAMS model used to estimate snowmelt induced erosion, Landschaftsgenese und Landschaftökologie, 16:7-8.

Botterweg, P.F. 1989. Utprovning og tilpassing av stofftapmodeller for landbruksarealer. GEFO rapport, Ås, Norge, 31 pp.

Botterweg, P.F. 1990. The effect of frozen soil on erosion - a model approach. In: Cooley, K.R. (ed.), Proceeding, International Symposium Frozen Soil Impacts on Agricultural, Range and Forest Lands, Spokane, Washington, 21-22 march 1990, CCREL Special Report 90-1, p 135-144

Destouni, G. 1991. Applicability of the Steady State Flow Assumption for Solute Advection in Field Soils. Water Resources Research, 27(8), 2129-2140.

Dressie, Z. 1987. Recharge and Soil Water Studies Using different Models and Measurement Methods. PhD thesis, Uppsala Universitet, Avd. f hydrologi, Rep A no 2 and 39

Eckersten, H. & Jansson, P-E. 1991. Modelling water flow, nitrogen uptake and production for wheat. Fertilizer Research 27:313-329.

Eckersten, H., Gärdenäs, A. & Jansson, P-E. 1995. Modelling Seasonal Nitrogen, Carbon, Water and Heat Dynamics of the Solling Spruce Stand. Ecological Modelling, 83: 119-129 .

Espeby, B. 1989. Water flow in a forested till slope. - field studies and physically based modelling. PhD thesis, Royal Institute of Technology, Dept. of Land and Water Resources, Rep. Trita-Kut No. 1052., 33 pp.

Espeby, B. 1992. Coupled simulations of water flow from a field-investigated glacial till slope using a quasi-two-dimensional water and heat model with bypass flow. Journal of Hydrology, 131:105-132.

Grip, H., Halldin, S., Jansson, P-E., Lindroth, A., Noren, B.,Perttu, K. 1979. Discrepancy between energy and water balance estimates of evapotranspiration. - In: S. Halldin (ed.) Comparison of Forest Water and Energy Exchange Models. Society for Ecological Modelling, Copenhagen, 237-255.

Gustafson, A. 1987. Water discharge and Leaching of Nitrate, PhD thesis, Sveriges Lantbruksuniversitet, Ekohydrologi 22.

Gustafson, A. 1987. Simulation of water discharge rates from a clay-till soil over a ten year period. Journal of Hydrology,92: 263-274.

Gärdenäs, A.I. & Jansson, P-E 1995. Simulated water balance of Scots pine stands in Sweden for different climate change scenarios. Journal of Hydrology, 166: 107-125.

Halldin, S.,Jansson, P-E.,Lundkvist, H. 1979. Ecological effects of long-term soil heat pump use. In: Proc. Nordic Symp. Earth Heat Pump Systems, Suppl. ,14-23. Gothenburg: Chalmers University of Technology

Halldin, S. 1980. SOIL water and heat model. I. Syntheses of physical processes. - Acta Universitatis Upsaliensis. Abstract of Uppsala Dissertations from the Faculty of Science 567, 26 pp.

Haugen, L-E., Jansson, P-E., Konovalov, N. & Uhlen G. 1991. Simulation of surface runoff and pipe drainage from a field lysimeter on cultivated soil at Ås, Norway, 1973-81. Norwegian Journal of Agricultural Sciences.

Iritz, Z., Lindroth, A. & A. Gärdenäs, 1997. Open ventilated chamber system for measurements of H_2O and CO_2 fluxes from soil surface. Soil Technology 10: 169-184

Jansson, P-E. 1980. SOIL water and heat model. II. Field studies and applications. - Acta Universitatis Upsaliensis. Abstract of Uppsala Dissertations from the Faculty of Science 568, 26 pp.

Jansson, P-E. 1981. SOIL water and heat model, applied to Möhlin forest. - Proc. from an IUFRO workshop in Birmensdorf, Switzerland, August 1979.12 pp.

Jansson, P-E. 1984. Vattnets passage genom den omättade zonen. i Proceedings från IHP symposium: Vattnet i det terrestra ekosystemet. NFR's kommitte för hydrologi, Rep. 58:43-54

Jansson, P-E. 1986. The Importance of Soil Properties when Simulating Water Dynamics for an Agricultural Crop-Soil System. Presented at the NHP-seminar on Water in the Unsaturated zone,

Jansson, P-E. 1987. Simulated soil temperature and moisture at a clearcutting in central Sweden. Scand. J. For. Res. 2:127-140

Jansson, P-E. 1987. SOIL water and heat model. Swedish University of Agricultural Sciences, Fakta no. 3, 4 pp.

Jansson, P-E. 1991. SOIL model. User's manual. Division of Agricultural Hydrotechnics, Communicatins 91:7, Swedish University of Agricultural Sciences, Uppsala. 69 pp.

Jansson, P-E. 1996. Water flows in Acid sulphate soils in Vietnam. A case study from Tan Tanh Farm. IRDCurrents, 43-46

Jansson, P-E. & Gustafson, A. 1987. Simulation of surface runoff and pipe discharge from an agricultural soil in northern Sweden, Nordic Hydrology 18:151-166

Jansson, P-E. & Halldin, S. 1979. Model for the annual water and energy flow in a layered soil. In: S. Halldin (ed.) Comparison of Forest and Energy Exchange Models. Society for Ecological Modelling, Copenhagen, 145-163.

Jansson, P-E. & Halldin, S. 1980. SOIL water and heat model. Technical description. - Swedish Coniferous Forest Project, Tech. Rep. 26, 81 pp. Uppsala: Swedish University of Agricultural Sciences

Jansson, P-E. & Reurslag, A. 1991. Climatic influence on litter decomposition: methods and some results on a NW-European transect. In: Jeffers, J. (ed.) Proceedings from First European Symposium on Terrestrial Ecosystems: Forests and Woodlands,Florence,20-24 May, 1991.

Jansson, P-E. & Thoms-Hjärpe, C. 1986. Simulated and measured soil water dynamics of unfertilized and fertilized barley. Acta Agric Scand 36:162-172.

Jansson,P-E. & Lundin L-C., 1984. Fysikaliska effekter av ytjordvärmeuttag. Simulerade uttag för olika marker och klimat. Byggforskningsrådet R50, 84s.

Jansson, P.-E., Stähli, M., Lindahl, A., Kellner, E. & Lundin, L.-C. 1995. Modelling of soil moisture dynamics and evaporation from two different forest stands at the NOPEX Central Tower Site. Annales Geophysicae 13, Suppl. II, p.C 342.

Johansson, P-O. 1986. Diurnal groundwater level fluctuations in sandy till - A model analysis. Journal of Hydrology, 87:125-134.

Johansson, P-O. 1987a. Estimation of ground water recharge in sandy till with two different methods using groundwater level fluctuations. Journal of Hydrology, 90:183-198.

Johansson, P-O. 1987b. Methods for estimation of direct natural groundwater recharge in humid climates - with examples from sandy till aquifers in southeastern Sweden. PhD thesis, KTH, Trita-Kut 1045.

Johnsson, H. & Jansson, P-E., 1991. Water balance and soil moisture dynamics of field plots with barley and grass ley. Journal of Hydrology, 129:149-173.

Johnsson, H. & Lundin, L-C. 1991. Surface runoff and soil water percolation as affected by snow and soil frost. Journal of Hydrology, 122:141-159.

Kätterer, T. & Andren, O. 1995 Measurements and simulations of heat and water balance components in a clay soil cropped with winter wheat under drought stress or daily irrigation and fertilization. Irrigation Science, 16:65-73.

Lee, Y.H. , Hultberg, H., Svedrup, H. & G. Ch. Borg, 1995. Are ion exchange processes important in controlling the cation chemistry of soil- and runoff waters? Water, Air and Soil Pollution 85: 1819-1824.

Lewan, E. 1993. Evaporation and discharge from arable land with cropped or bare soil during winter. Measurements and simulations. Agricultural and forest meteorology, 64:131-159.

Lewan, E. 1994. Effects of a catch crop on leaching of nitrogen from a sandy soil: Simulations and measurements. Plant and Soil, 166:137-152.

Lewan, L. 1996. Evaporation, Discharge and Nitrogen Leaching from a Sandy Soil in Sweden. Simulations and Measurements at Different Scales in Space and Time. Swedish University of

Agricultural Sciences. Department of Soil Sciences. Reports and Dissertations 27, 27p. + 4 papers

Lewan, E. & Jansson, P.-E. 1996. Imblications of spatial variability of soil physical properties for simulation of evaporation at the field scale, WRR vol. 32, pp. 2067-2074.

Lundin, L-C. 1985. Simulated physical effects of shallow soil heat extraction. Cold Reg. Sci. Tech. 11:45-61.

Lundin, L-C. 1989. Water and heat flows in frozen soils. Basic theory and operational modeling. Acta Univ. Ups., Comprehensive Summaries of Uppsala Dissertations from the Faculty of Science 186. 50 pp. Uppsala

Lundin, L-C. 1990. Simulating the freezing and thawing of arable land in Sweden, In: Cooley, K.R. (ed.), Proceeding, International Symposium Frozen Soil Impacts on Agricultural, Range and Forest Lands, Spokane, Washington, 21-22 march 1990, CCREL Special Report 90-1, p 87-98

Lundin, L-C. 1990. Hydraulic properties in an operational model of frozen soil. Journal of Hydrology 118:289-310.

Lundin, L-C. & Johnsson, H. 1990. Modelling infiltration of snow melt water into frozen soils, In: Sigurdsson, G. (ed.), Nordic Hydrological Conference 1990. Nordisk NHP-rapport nr 26, Norrköping, pp. 53-62.

McGechan, M. 1994. A model of the economics and environmental impacts of alternative animal waste management systems. Proc. International Conefencenc AGENG 94, Milan, 29-31 August, 1088-1095.

McGechan, M. & Cooper, G. Workdays for winter field operations. The Agricultural Engineer, 1994, 49: 6-13.

McGechan, M.B., Graham, R., Vinten, A.J.A., Douglas, J.T. and Hooda, P.S., 1997. Parameter selection and testing the soil water simulation model SOIL. Journal of Hydrology 195, 312-344.

McGechan, M.B. and Wu, L., 1998. Environmental and economic implications of some slurry management options. Journal of Agricultural Engineering Research (in press).

Nordén, L.G. 1989. Water use by Norway spruce - a study of two stands using field measurements and soil water modelling. PhD thesis, Dept. of Forest Site Research, Swedish University of Agricultural Sciences. 43 pp.

Persson, G. 1995. Water balance of willow Stands in Sweden. Field Studies and Model Applications. . Swedish University of Agricultural Sciences. Department of Soil Sciences. Reports and Dissertations 20, 27p. + 5 papers

Persson, G. 1997. Comparison of simulated water balance for willow, spruce, grass ley and barley. Nordic Hydrology, 28, pp. 85-89.

Persson, G. & Jansson, P-E. 1989. Simulated water balance of a willow stand on a clay soil. In: Simulation of Growth and Profitability of a Willow Energy Forest, Kowalik, P. & Perttu, K. (eds), Wageningen, pp. 147-162.

Persson, G & Lindroth, A. 1994. Simulating evaporation from short-rotation forest: variations within and between seasons. Journal of Hydrology 156: 21-45

Seip, K.L. & Botterweg, P.F. 1988. User's experiences and the predictive power of sediment yield and surface runoff models. Proceedings of the International Symposium on watr quality modeling of argricultural non-point sources. 1988, Utah State University, Logan, Utah, Donn. G. Decoursey (ed). ARS-81, pp-205-224.

Stadler, D, Flühler, H., Jansson, P-E. 1997. Modelling vertical and lateral water flow in frozen and sloped forest soil plots. Cold Region Science and Technology 26: 181-194.

Stähli, M., Jansson, P.-E. & Lundin, L.-C. 1995. Preferential water flow in partly frozen soil - a two-domain model approach, in: Krauss, T.W. & Carroll, T.R. International GEWEX Workshop on Cold-Season/Region Hydrometeorology, Summary Report and Proceedings, Banff, Alberta, Canada, 22-26 May 1995, IGPO Publication Series No.15.

Stähli, M. & Jansson, P.-E. 1998. 'Test of two SVAT snow submodels during different winter conditions', accepted for publication Agricultural and Forest Meteorology.

Troedsson, T.,Jansson, P-E., Lundkvist, H., Lundin, L., Svensson, R. 1982. Ekologiska effekter av ytjordvärmeuttag. Markkemi, markfysik, markbiologi, markhydrologi och växtodling. Byggforskningsrådet ,Stockholm, 76 pp.

Thunholm, B., Lundin, L-C., Lindell, S. 1989. Infiltration into a frozen heavy clay soil. Nordic Hydrology, 20: 153-166.

Thunholm, B. 1990. Temperature and Freezing in Agricultural Soils as Realted to Soil Properties and Boundary Conditions. PhD Thesis, Swedish University of Agricultural Sciences, Dept of Soil Sciences, Reports and Dissertations: 7, 26 p.

Thunholm, B. 1990. A comparison of measured and simulated soil temperature using air temperature and soil surface energy balance as boundary conditions. Agricultural and Forest Meteorology, 53:59-72.

Thunholm, B. & Lundin, L-C. 1990. Infiltration into a seasonally frozen soil, In: Cooley, K.R. (ed.), Proceeding, International Symposium Frozen Soil Impacts on Agricultural, Range and Forest Lands, Spokane, Washington, 21-22 march 1990, CCREL Special Report 90-1, p 156-160

Wu, L. and McGechan, M.B., 1998a. A review of carbon and nitrogen processes in four soil nitrogen dynamics models. Journal of Agricultural Engineering   Research (in press).

Wu, L., McGechan, M.B., Lewis, D.R., Hooda, P.S. and Vinten, A.J.A., 1998. Parameter selection and testing the soil nitrogen dynamics model SOILN.   Soil Use and Management (in press).

Wu, L. and McGechan, M.B., 1998b. Simulation of biomass, carbon and nitrogen accumulation in grass to link with a soil nitrogen dynamics model. Grass and Forage Science (in press).

Förteckning över utgivna häften i publikationsserien

SVERIGES LANTBRUKSUNIVERSITET, UPPSALA. INSTITUTIONEN FÖR MARKVETENSKAP.
AVDELNINGEN FÖR LANTBRUKETS HYDROTEKNIK. AVDELNINGSMEDDELANDE. Fr o m 1995

95:1   Alavi, G. Radial stem growth and transpiration of Norway spruce in relation to soil water availability. Granens
         tillväxt och transpiration i relation till markvattnets tillgänglighet (Licenciatavhandling). 13 + 11 + 14 s.

95:2   Johansson, W. & Fellin, O. Biogas från vall. Teknik och ekonomi vid odling, skörd, transporter, ensilering
         samt rötning med tvåstegsteknik. 38 s.

95:3   Svensson, E., Linnér, H. & Carlsson, H. Utvärdering av växtanalys i fabrikspotatis. 53 s.

95:4   Andersson, A. Vattentillgångar för bevattning i Kalmar län. I. Litteraturöversikt. II. Intervjuundersökning rörande
         vattenmagasin. 48 s.

95:5   Wesström, I. Bestämning av markens salthalt genom mätning med konduktivitetssond. 18 s.

95:6   Eckersten, H., Jansson, P-E., Karlsson, S., Persson, B., Perttu, K. & Andersson, J. En introduktion till
         biogeofysik. 72 s.

95:7   Eckersten, H. Simulation of water flow in plant communities. SPAC model description, exercises and user's
         manual. 49 s.

95:8   Nabieian, F. Simulering av vattenbalans för energiskog på en torvmark. 25 s.

96:1   Eckersten, H., Jansson, P-E., & Johnsson, H. SOILN model, user's manual. Version 9.1. 93 s.

96:2   Eckersten, H., Jansson, P-E., Karlsson, S., Lindroth, A., Persson, B., Perttu, K. & Andersson, J. En introduktion
         till biogeofysik, 2:a upplagan. 110 s.

96:3   Carlsson, H., Larsson, K. & Linnér, H. Växtnäringsstyrning i potatis. 69 s.

97:1   Uppenberg, S., Wallgren, O. & Åhman, M. Saturated hydraulic conductivity in an acid sulphate soil. A minor
         field study in the the Vietnamese Mekong delta. 45 s.

97:2   Djodjic, F. Avrinningsmönster i ett litet åkerområde under 40 år av successiv urbanisering. 38 s.

97:3   Vukovic, M. The effect of soil hydraulic properties on ground water fluctuations in a heavy clay soil.
         Measurements and simulations. 43 s.

97:4   Eckersten, H., Jansson, P-E., Karlsson, S., Lindroth, A., Persson, B., Perttu, K., Carlsson, M., Lewan, L. &
         Blombäck, K. En introduktion till biogeofysik, 3:e upplagan. 130 s.

97:5   Eckersten, H. Simulation of water flow in plant communities. SPAC model description, exercises and user's
         manual. 2nd edition. SPAC version 5.0. 52 s.

98:1   Lustig, T. Land Evaluation Methodology. Small-Scale Agro-Pastoralist Farming Systems. Agricultural
         community case study in the IV region of Chile. 91 s.

98:2   Jansson, P-E. Simulating model for soil water and heat conditions. Description of the SOIL model. 81 s.